HHS Public Access

Author manuscript

Nat Microbiol. Author manuscript; available in PMC 2024 December 01.

Published in final edited form as:

Nat Microbiol. 2024 June ; 9(6): 1607–1618. doi:10.1038/s41564-024-01697-8.

Propionate prevents loss of the PDIM virulence lipid in *Mycobacterium tuberculosis*

Claire V. Mulholland,
Thomas J. Wiggins[†],
Jinhua Cui[†],
Catherine Vilchèze,
Saranathan Rajagopalan,
Michael W. Shultis,
Esmeralda Z. Reyes-Fernández,
William R. Jacobs Jr,
Michael Berney[*]

Department of Microbiology and Immunology, Albert Einstein College of Medicine, Bronx, New York, USA

Abstract

Phthiocerol dimycocerosate (PDIM) is an essential virulence lipid of *Mycobacterium tuberculosis*. *In vitro* culturing rapidly selects for spontaneous PDIM-negative mutants, which have attenuated virulence and increased cell wall permeability, thus impacting the relevance of experimental findings. PDIM loss can also reduce efficacy of the BCG Pasteur vaccine. Here, we show that vancomycin susceptibility can rapidly screen for *M. tuberculosis* PDIM production. We find that metabolic deficiency of methylmalonyl-CoA impedes the growth of PDIM-producing bacilli, selecting for PDIM-negative variants. Supplementation with odd-chain fatty acids, cholesterol, or vitamin B_{12} restores PDIM-positive bacterial growth. Specifically, we show that propionate supplementation enhances PDIM-producing bacterial growth and selects against PDIM-negative mutants, analogous to *in vivo* conditions. Our study provides a simple approach to screen for and

[*]Corresponding author.: michael.berney@einsteinmed.edu.

Author contributions

C.V.M. and M.B. conceived and designed the study. C.V.M., T.J.W., J.C., C.V., S.R., M.W.S., and E.Z.R., performed the experiments. C.V.M., T.J.W., C.V., M.W.S., and M.B. analysed the data. M.B. and W.J.R. provided resources. C.V.M. and M.B. wrote the paper. T.J.W., C.V., S.R., M.W.S., E.Z.R., and W.J.R. critically reviewed and edited the paper.

[†]These authors contributed equally to this work

Code availability statement

WGS data were processed on the Albert Einstein College of Medicine High-Performance Computing Core (HPC). Scripts used for reference-guided assembly and variant calling are available at https://github.com/cvmulholland/MtbShortReadWGS.

Competing interests

C.V.M. and M.B. are inventors on a pending patent related to this work (U.S. Patent Application No. 63/527,831, filed 20 July 2023). The authors declare that they have no other competing interests. The remaining authors declare no competing interests.

Additional information

Supplementary Information is available for this paper.

Correspondence and requests for materials should be addressed to Michael Berney.

maintain PDIM production, and reveals how discrepancies between the host and *in vitro* nutrient environments can attenuate bacterial pathogenicity.

Introduction

The cell wall of *Mycobacterium tuberculosis* (*Mtb*) is exceptionally complex and is essential to its success as a pathogen. Phthiocerol dimycocerosates (PDIMs) are long-chain non-polar lipids found in the outermost layer of the cell wall of *Mtb* and other pathogenic slow-growing mycobacteria[1]. PDIMs play a crucial role in *Mtb* pathogenesis (reviewed in[2]), however, *Mtb* is prone to losing the ability to produce PDIM *in vitro* due to spontaneous mutation of PDIM biosynthesis genes[3,4]. Loss of PDIM biosynthesis confers a growth advantage in current mycobacterial culture media[3,5], resulting in PDIM-deficient mutants dominating cultures with successive passage[3]. As PDIM deficiency decreases virulence[5–11] and increases cell wall permeability[12,13], spontaneous PDIM loss adversely affects experimental reliability, reproducibility, and the interpretation of results. PDIM deficiency has also been shown to reduce the vaccine efficacy of *Mycobacterium bovis* BCG Pasteur[14]. “The PDIM problem” thus presents a major challenge in tuberculosis research and has hindered progress in the field for decades. The genetically unstable nature of the PDIM biosynthetic pathway makes routine PDIM screening essential for all branches of tuberculosis research. However, current PDIM screening approaches such as whole genome sequencing (WGS), mass spectrometry, and thin layer chromatography (TLC), are expensive, cumbersome, and require specialized equipment and expertise, further compounding the PDIM problem.

We sought to understand the underlying cause of PDIM loss and develop routine methods to enable reproducible PDIM bias-free investigations in all branches of *Mtb* research. Here we developed a facile and scalable routine assay for PDIM production and a modified culture media that maintains PDIM production. We show that in standard culture media, the growth of PDIM-producing bacilli is impaired due to MMCoA deficiency. Supplementation with propionyl-CoA-generating carbon sources or vitamin B_{12} restores the growth of PDIM-producing *Mtb*, eliminating the selective advantage of PDIM loss. Propionate supplementation was found to select against PDIM-negative mutants enabling the maintenance of pure PDIM-positive cultures. Furthermore, we show that propionate supplementation enhances PDIM-dependent drug resistance, directly linking propionyl-CoA metabolism and PDIM production with enhanced rifampicin resistance.

Results

Vancomycin sensitivity can screen for PDIM phenotype

We hypothesized that the differential permeability of PDIM-positive [PDIM(+)] and PDIM-negative [PDIM(-)] *Mtb*[12,13] could be exploited to develop a simpler functional PDIM assay. To test this, we first assembled a PDIM reference strain set comprised of six BSL2-approved attenuated *Mtb* H37Rv strains with varying PDIM content (Fig. 1a, Supplementary Table 1). These strains demonstrate the heterogeneity of PDIM production commonly found in laboratory *Mtb* strains. Vancomycin – a large antimicrobial glycopeptide not normally

used for *Mtb* treatment due to poor penetration, has previously been reported to be more effective against PDIM deletion mutants of *Mtb* and *M. bovis* BCG than the corresponding PDIM(+) wildtype strains[15]. Accordingly, we found that PDIM levels measured by TLC significantly correlated with vancomycin MIC_{90} and MIC_{50} in our reference strain set after 10–14 days of incubation (Supplementary Fig. 1). PDIM(+) *Mtb* $mc^2$7902 was also more resistant to other high molecular weight compounds than PDIM(-) $mc^2$8398, though vancomycin gave the best differentiation (Extended Data Fig. 1a-g). Furthermore, much greater Ethidium Bromide uptake[16] was observed in $mc^2$8398 than $mc^2$7902 (Extended Data Fig. 1h), consistent with enhanced permeability of PDIM(-) strains.

Whilst an intact biosynthetic pathway is essential for PDIM production, PDIM size and abundance are dependent on the availability of the precursor methylmalonyl-CoA (MMCoA)[17]. MMCoA is generated from propionyl-CoA by propionyl-CoA carboxylase, or, from succinyl-CoA by vitamin B_{12}-dependent MMCoA mutase (Fig. 1b). In the host, *Mtb* has access to propionyl-CoA-generating carbon sources such as cholesterol[18,19] and possibly also scavenges vitamin B_{12}[20-22]. Standard Middlebrook 7H9/OADC/glycerol media, however, lacks both a propionyl-CoA-generating carbon source and vitamin B_{12}. Propionate supplementation or growth on cholesterol have been shown to increase the biosynthesis of PDIM and other virulence lipids[17,19,23,24]. Accordingly, we found that the addition of 0.1 or 1.0 mM propionate preferentially increased vancomycin resistance of PDIM(+) strains in 7H9/OADC/glycerol/tyloxapol + PALM media (pantothenate, arginine, leucine, and methionine; for BSL2 auxotrophic strains), enhancing the differentiation between PDIM(+) and PDIM(-) *Mtb* while improving assay robustness and reducing time to result (Fig. 1c, and Extended Data Fig. 2). To further simplify our approach and enable scalability, we established a single concentration assay we term the ‘VAN10-P assay’ (Fig. 1e, Extended Data Fig. 2c and Supplementary Fig. 2). This compares growth in 10 μg/ml vancomycin with 0.1 mM propionate to no-drug controls and highly correlates with PDIM production (Fig. 1f). We additionally validated our approach using PDIM(-) (Δ*ppsD*) and complemented (Δ*ppsD*::comp) strains constructed from a PDIM(+) clone (H37Rv-SC, wildtype) (Supplementary Table 2). PDIM(+) and PDIM(-) H37Rv showed a >30-fold difference in vancomycin MIC_{90} with 0.1 mM propionate (‘VAN-P’ MIC) (Fig. 1g) and this was also reflected in the VAN10-P assay (Fig. 1h). Highly similar results were also obtained for *Mtb* CDC1551 and its PDIM(-) (Δ*mas*) mutant (Supplementary Fig. 3).

To confirm that increased vancomycin resistance with propionate was due to enhanced PDIM production rather than other effects such as accumulation of propionyl-CoA or methylcitrate cycle intermediates[25,26], we supplemented with vitamin B_{12} to provide an alternate route for MMCoA production via the vitamin B_{12}-dependent methylmalonyl pathway[22] (Fig. 1b). Vitamin B_{12} selectively increased the vancomycin resistance of PDIM(+) *Mtb* mirroring the effect of propionate (Fig. 1g and Extended Data Fig. 2b,c), consistent with enhanced resistance due to increased PDIM production. Co-supplementation with both propionate and vitamin B_{12} had comparable effects to each on its own (Supplementary Fig. 4), indicating the activation of either pathway provides sufficient precursors for PDIM biosynthesis at the concentrations tested. The branched-chain amino leucine did not have a marked effect on vancomycin resistance at the concentration provided in PALM-supplemented media (Supplementary Fig. 5a). Whilst degradation of branched-

chain amino acids provides a potential source of propionyl-CoA, the end products of leucine catabolism are in fact acetyl-CoA and acetoacetate[27], likely explaining the failure of this to phenocopy propionate supplementation.

As Tween 80 is another detergent commonly used in *Mtb* culture media we tested whether tyloxapol could be replaced with Tween 80 in our assay. Tween 80 is known to remove several layers of the mycobacterial cell wall including PDIM[28]. Consistent with this, Tween 80 abolished PDIM-related differences in vancomycin resistance and further increased the vancomycin sensitivity of PDIM(-) *Mtb* (Fig. 1h and Extended Data Fig. 3).

Prevalence of PDIM loss across *Mtb* strains

Next, we determined the predictive power of our approach in a range of virulent *Mtb* strains including Erdman, HN878, KZN 4207, and two different CDC1551 and H37Rv stocks (Supplementary Table 2). VAN-P screening reliably predicted PDIM levels as determined by TLC for all these strains (Fig. 2a and Extended Data Fig. 4a–d). Furthermore, VAN-P assays outperformed WGS at diagnosing PDIM deficiencies in heterogeneous populations. TLC and VAN10-P assays showed low PDIM levels in H37Rv-A and CDC1551-A (Fig. 2a), however, standard WGS variant calling failed to identify any PDIM mutations in these stocks, whilst an unfixed mutation was identified in Erdman (Supplementary Table 3). Low-frequency variant analysis subsequently identified putative PDIM mutations at ~10–13% frequency in each of these stocks (Supplementary Table 4), indicating they comprise a mixture of different PDIM(-) mutants. Thus, WGS is a poor predictor of PDIM levels in mixed populations as these can comprise an array of different low-frequency PDIM mutations, which can be difficult to detect by WGS.

To investigate how genetic engineering of *Mtb* strains is affected by PDIM loss we generated knockout mutants of the non-PDIM-related gene *tgs1* from a mouse-passaged H37Rv stock (H37Rv-B) using specialized transduction[29]. Surprisingly, despite this being an animal-passaged stock, only one of eight Δ*tgs1* mutants obtained (Δ*tgs1*-7) was found to be fully PDIM(+) by VAN-P MICs (Fig. 2b). This was further validated by TLC and sequence analysis (Fig. 2c, Supplementary Table 3). Δ*tgs1*-1 and Δ*tgs1*-4 were deemed PDIM-deficient by our assay and harbor non-synonymous PDIM SNPs yet showed PDIM bands by TLC. Both, however, display altered band patterns and lower overall PDIM abundance compared to the fully PDIM(+) Δ*tgs1*-7 mutant. This highlights the sensitivity of our approach to detect PDIM biosynthetic defects that do not fully eliminate PDIM production but have phenotypic consequences.

Historically animal passaging was the only procedure known to select for PDIM(+) *Mtb*. However, our results suggested that despite animal passage H37Rv-B may still be a mixed population (Fig. 2a–c). Indeed, VAN10-P single colony screening confirmed that while animal passage enriched for PDIM(+) clones, PDIM-deficient strains were not completely removed (Fig. 2d, Supplementary Table 3). Consequently, using VAN10-P single colony screening, we were able to isolate single PDIM(+) clones from H37Rv-B, as well as other virulent strains and avirulent mc^{2}6230 (Extended Data Fig. 4 and Supplementary Table 3).

Strikingly, six different mutations in five different PDIM genes were identified across the seven PDIM(-) Δ*tgs1* mutants (Fig. 2e), emphasizing the genetic heterogeneity in the PDIM gene cluster in mixed populations. We also found two unique frameshift mutations in a 7-cytosine homopolymeric tract in *ppsC* (Extended Data Fig. 5). This region appears to be a 'hotspot' for mutation as we also found *ppsC* homopolymeric tract mutations in $mc^2$6230 (Supplementary Tables 3 and 5) and in the literature[30,31]. Homopolymeric tracts are prone to mutations caused by slipped-strand mispairing[32] and as *Mtb* lacks a DNA mismatch repair system[33] this may lead to hypervariability in these regions, further augmenting the propensity for PDIM loss *in vitro*.

Collectively these data validate VAN-P assays as a reliable and effective method to assess PDIM levels and heterogeneity in *Mtb* populations and aid isolation of PDIM(+) clones. However, the data presented also strongly emphasized the need to resolve the underlying issue of PDIM loss.

Increased MMCoA availability restores growth of PDIM(+) *Mtb*

As PDIM production is tightly coupled to *Mtb* metabolism[17], we reasoned that there may be a metabolic solution to the PDIM problem. Propionyl-CoA, an upstream precursor of PDIM, can be inhibitory to bacterial growth[34]. The major pathways for propionyl-CoA detoxification are the methylcitrate cycle[35], the methylmalonyl pathway[22], and the incorporation into PDIM and other virulence-associated lipids[36,37] (Fig. 1b). We hypothesized that PDIM-deficient strains would be more sensitive to propionate toxicity without this sink for propionyl-CoA metabolism and that this could be exploited to create a PDIM selective medium. Accordingly, the PDIM(-) strains in our reference strain set were more sensitive to propionate than the PDIM(+) (Fig. 3a). Surprisingly, we also observed that PDIM(+) strains reached higher density at lower propionate concentrations (Fig. 3a), suggesting sub-toxic propionate may provide a growth advantage to PDIM(+) *Mtb*.

Next, we compared the growth of PDIM(+) and PDIM(-) *Mtb* with propionate and other supplements. Notably, we found that the addition of 0.1 or 1.0 mM propionate to standard 7H9/OADC/glycerol/tyloxapol media increased the growth rate of PDIM(+) strains to that of PDIM(-) (Fig. 3b and Extended Data Fig. 6b,c). Again, we did not observe comparable effects when tyloxapol was replaced with Tween 80 (Extended Data Fig. 6k–m). The odd-chain fatty acid valerate also restored PDIM(+) growth, but not the even-chain fatty acids acetate or butyrate, or the three-carbon metabolite pyruvate (Extended Data Fig. 6g–j), demonstrating this effect is specific to propionyl-CoA generating carbon sources. Supplementing with cholesterol not only restored PDIM(+) growth but also significantly reduced the growth of PDIM(-) *Mtb* (Fig. 3c). The growth reduction of PDIM(-) *Mtb* is likely related to the reduced ability to maintain redox homeostasis via lipid anabolism[37], a mechanism induced during cholesterol catabolism[38]. Importantly, vitamin B_{12} also restored PDIM(+) growth analogous to propionate (Fig. 3b). Taken together, these data indicate that in standard media PDIM(+) growth is impaired due to a deficiency of MMCoA. This is consistent with previous work showing that vitamin B_{12} enhances the growth of wildtype H37Rv but not of a methylmalonyl-CoA mutase deletion mutant[22]. This was further supported by measuring the intracellular abundance of MMCoA by LC-MS. In

unsupplemented media, MMCoA levels in PDIM(+) *Mtb* were approximately 3-fold lower than in PDIM(-), but increased to similar levels with propionate supplementation (Fig. 3d). Vitamin B_{12} supplementation also significantly increased MMCoA but not propionyl-CoA levels in PDIM(+) *Mtb* (Fig. 3e and Extended Data Fig. 7a), supporting the notion that MMCoA deficiency specifically is responsible for the growth retardation in PDIM(+) *Mtb*.

Propionate and vitamin B_{12} maintain PDIM production

Based on these findings, we reasoned that propionate supplementation would prevent PDIM loss by eliminating the growth advantage of PDIM(-) cells. Whilst arguably cholesterol could also be used for this purpose, propionate is both more affordable and much simpler to work with as a routine media supplement. To assess this, we performed *in vitro* experimental evolution using culture stocks with different PDIM(+) to PDIM(-) ratios. First, we serially passaged H37Rv-B – a moderately PDIM(+) mixed population (Fig. 2d), by weekly subculture in 7H9/OADC/glycerol/tyloxapol ± 0.1 or 1.0 mM propionate and assessed PDIM levels by TLC and VAN10-P assays. Considerable PDIM loss was observed in unsupplemented media whereas propionate supplementation fully maintained PDIM production (Fig. 4a). Repeating this experiment starting from a fully PDIM(+) clone, we saw a marked decline in PDIM in unsupplemented media after five passages, whilst 0.1 mM propionate maintained PDIM production for the duration of the experiment (Extended Data Fig. 8c). Strikingly, starting from H37Rv-A – a predominantly PDIM(-) population, PDIM levels progressively increased with propionate (Fig. 4b). VAN10-P screening of single colonies confirmed enrichment of PDIM(+) clones (Fig. 4c), demonstrating 0.1 mM propionate positively selects for PDIM-producing *Mtb*. We speculated that whilst advantageous for the growth of PDIM(+) *Mtb*, 0.1 mM propionate selects against PDIM(−) cells due to propionyl-CoA toxicity[39] in the absence of a functional PDIM biosynthetic pathway. Indeed, the addition of vitamin B_{12} to alleviate propionyl-CoA toxicity via activation of the methylmalonyl pathway[22,36] considerably slowed the selection process and resembled more cultures with vitamin B_{12} alone (Fig. 4d and Extended Data Fig. 8d,e). This represents an important advance for the tuberculosis field as it demonstrates that propionate improves the growth of PDIM(+) cells and provides a competitive advantage against spontaneous PDIM(-) mutants, thereby enabling the maintenance of pure PDIM(+) *Mtb* cultures *in vitro*.

Propionate increases PDIM-dependent drug resistance

As PDIM levels had such a profound effect on vancomycin resistance, we sought to further explore the impact of propionate supplementation on drug resistance. MIC assays of several first- and second-line antitubercular drugs revealed that propionate significantly increased resistance to rifampicin and bedaquiline in a PDIM-dependent manner, while smaller inhibitors like isoniazid, linezolid, and pretomanid showed no difference (Fig. 5 and Supplementary Figs. 6 and 7). Vitamin B_{12} mirrored the effects of propionate supplementation on rifampicin and bedaquiline resistance (Fig. 5a,c), consistent with enhanced resistance due to increased PDIM production. Notably, the rifampicin MIC_{90} for PDIM(+) *Mtb* in propionate-supplemented media reduced ~30-fold when tyloxapol was replaced with Tween 80 (Fig. 6). These data are also congruent with our earlier results showing greater resistance of PDIM(+) *Mtb* to large compounds and lower permeability

compared to PDIM(−) (Extended Data Fig. 1). One outlier to this trend was capreomycin (668.7 g/mol), which did not exhibit a PDIM-propionate MIC shift (Supplementary Fig. 6a). Wang *et al.* have also reported PDIM-dependent resistance to the small molecule inhibitor 3bMP1 (229.3 g/mol)[12], indicating that the relationship between the PDIM permeability barrier and drug uptake is complex though the uptake of large compounds is more likely to be affected by PDIM.

Discussion

The mycobacterial cell wall plays a crucial role in the interactions between the pathogen and host[40]. However, the study of *Mtb* cell wall biology and pathogenesis has long been impeded by heterogeneity in PDIM production. It has been nearly 50 years since the first report to associate PDIM loss with *in vivo* virulence attenuation[8], and over 20 years since PDIM loss and virulence attenuation were linked at the genetic level[6,7]. Numerous studies have since reported spontaneous PDIM loss not only in *Mtb* H37Rv[3–5,12], but also in *Mtb* Erdman[41,42], HN878[3], CDC1551[30,43], and in BCG vaccine strains[44]. This issue of spontaneous loss of PDIM production is thus both long-standing and far-reaching. The number of studies unpublished due to PDIM bias and the time and resources spent chasing PDIM-related phenotypes are likely to be high[5,41,42].

We discovered that *Mtb* metabolism affects the selective pressures to maintain PDIM(+) phenotypes. *Mtb* growth is impaired in the absence of an exogenous source of MMCoA precursors, which is required to produce PDIM and other methyl-branched lipids. PDIM loss increases the MMCoA pool and confers a growth advantage against PDIM(+) bacilli, providing a selective pressure for PDIM loss. This can be alleviated by supplementing propionyl-CoA-generating carbon sources such as odd-chain fatty acids or cholesterol, or the cofactor vitamin B_{12}, which increase MMCoA pools and restore full growth of PDIM(+) *Mtb*. The affinity of *Mtb* for host fatty acids was first described by Segal and Bloch in 1956[45] and we now know that *Mtb* also metabolizes host cholesterol[18]. Cholesterol is thought to be a major source of propionyl-CoA in the host[19], and *Mtb* has evolved to efficiently use this host-derived sterol resource as fuel for cellular metabolism and a building block for virulence lipids[18,36]. Moreover, starving the bacterium of propionyl-CoA via cholesterol limitation improves macrophage control of *Mtb*[46], demonstrating a crucial role for this metabolite in *Mtb* during infection. *Mtb* culture media is, however, devoid of propionyl-CoA precursors. We speculate that the toxicity of high concentrations of odd-chain fatty acids previously discouraged their inclusion, as most *Mtb* culture media were optimized to promote rapid planktonic growth rather than to reflect the nutrient environment found in the host[47,48]. Contrary to its negative reputation, we show that 0.1–1.0 mM propionate is advantageous for PDIM(+) growth and selects against PDIM(-) cells, analogous to animal passage, providing an elegant and long-sought solution to prevent loss of PDIM production. Our data also demonstrate that tyloxapol and not Tween 80 should be used in PDIM assays and PDIM selective media, as tyloxapol maintains PDIM-dependent impermeability, whilst Tween 80 strips PDIM and other cell wall components from the *Mtb* cell envelope[28].

Our data also may have ramifications for future drug discovery efforts. During host infection, *Mtb* survives in a PDIM-rich state[17], however, PDIM production is poorly supported in current culture media. We show that PDIM levels affect the potency of rifampicin, bedaquiline and other high molecular weight inhibitors, with reduced PDIM production increasing *Mtb* sensitivity to these compounds. In concert with the current literature[24,49,50], this clearly points to the mycobacterial cell wall as an important factor in drug efficacy and suggests that PDIM loss might lead to overestimation of drug potency.

Furthermore, our observation of increased vancomycin and rifampicin sensitivity of *Mtb* grown in Tween 80 containing media, confirms previous reports [51,52], and advocates for the use of tyloxapol to maintain the natural permeability barrier in *Mtb*. Our findings also expand on previous observations associating propionyl-CoA metabolism with rifampicin resistance[24,26] by directly linking propionyl-CoA and PDIM production with enhanced rifampicin resistance. The decreased virulence and increased drug sensitivity of PDIM(-) *Mtb* suggest that inhibitors of PDIM biosynthesis could increase the *in vivo* potency of current drug regimens. Although speculative, such a therapeutic option would likely be highly specific, as PDIMs are confined to slow-growing, pathogenic mycobacteria. Furthermore, inhibitors targeting propionyl-CoA metabolism could be synergistic with rifampicin due to downstream effects on PDIM.

The main recommendations stemming from our study are to routinely supplement culture media with 0.1–1.0 mM propionate and avoid Tween 80 to prevent PDIM loss and the emergence of populations with heterogeneous PDIM production. In mixed populations, standard media will select for PDIM(-) bacilli while propionate-supplemented media will select for PDIM(+) bacilli. To prevent these dynamic population changes and variation within or between cultures, we recommend always working with purified cultures maintained in the appropriate media. Our discoveries facilitate the maintenance and surveillance of PDIM production and enable efficient re-isolation of PDIM(+) strains from mixed populations. Pure and appropriately maintained PDIM(+) strains will be indispensable for studying bacterial virulence, interactions with host immunity[5,53], as well as for pre-clinical work such as vaccine studies. Moreover, today in the emerging era of *Mtb* systems biology where large pools of genetically modified strains are crucial tools for *in vitro* and *in vivo* studies[55–56], preventing secondary PDIM mutations is imperative to prevent potential misattribution of phenotypes to genotypes. Importantly, this approach is accessible to everyone, including labs in low-resource settings.

Taken together, our findings resolve the basis for selection of PDIM(−) *Mtb*. They also reveal how discrepancies between the host and *in vitro* nutrient environments can influence bacterial pathogenicity, and provide tools and culture conditions to maintain *Mtb* PDIM production to improve reliability in tuberculosis research.

Methods

Bacterial strains, culture condition and reagents

Mtb strains were obtained from laboratory stocks and are listed in Supplementary Tables 1 and 2. Fresh starter cultures were inoculated from frozen seed stocks and then subcultured

once before use in experiments. Subcultures were typically grown for four days to an optical density (OD) at 600 nm (OD_{600}) of ~0.8. For BSL2 strains, OD_{600} was measured using a GENESYS 140 spectrophotometer (Thermo Fisher Scientific). For BSL3 strains, OD_{600} was measured on a Biowave WPA CO8000 spectrophotometer (Biochrom Ltd.) and then converted using a calibration curve constructed against a GENESYS 10uv spectrophotometer (Thermo Fisher Scientific). Preculturing steps were performed using Middlebrook 7H9 broth supplemented with 10% (v/v) OADC (0.6 g/l sodium oleate, 50 g/l bovine serum albumin fraction V, 20 g/l dextrose, 40 mg/l catalase, 8.5 g/l sodium chloride), 0.2% (v/v) glycerol, and 0.05% (v/v) tyloxapol. This is referred to as standard 7H9/OADC/glycerol/tyloxapol media. BSL2 strains (Supplementary Table 1) were additionally supplemented with 24 mg/l D-calcium pantothenate, 200 mg/l L-arginine, 50 mg/l L-leucine, and 50 mg/l L-methionine ('PALM' supplements). Hygromycin B at 75 μg/ml and kanamycin at 30 μg/ml were added to precultures as indicated (Supplementary Table 2). For supplemented media, 1000 × supplement stocks were prepared in MilliQ water, filter sterilized, then added to standard media and the pH checked. Final supplement concentrations were as follows: 0.1 mM or 1.0 mM sodium propionate, 7.4 μM vitamin B_{12} (10 μg/ml), and 0.1 mM sodium pyruvate, sodium acetate, sodium butyrate and valeric acid. Cholesterol was prepared at 0.1 M in 1:1 (v/v) EtOH/tyloxapol as previously described[36] and then added to detergent-free media to give a final concentration of 0.1 mM cholesterol and 0.05% tyloxapol. Controls were prepared by adding EtOH/tyloxapol in the same manner to provide the detergent. For Tween 80 experiments, 0.05% Tween 80 was used in place of tyloxapol. For growth curve experiments, triplicate inkwells with 5 ml of media were inoculated at a starting OD_{600} of 0.01. Broth cultures were grown at 37 °C with gentle shaking (100 rpm for BSL2 strains, 80 rpm for BSL3). Middlebrook 7H10 agar supplemented with 10% (v/v) OADC and 0.5% (v/v) glycerol (7H10/OADC/glycerol) was used as a solid media for plating and plates were incubated at 37 °C for three weeks. Supplier information for media components and supplements are listed in Supplementary Table 6.

Mutant generation and complementation

Deletion of the *tgs1* (*Rv3130c*), *ppsD* (*Rv2934*) and *mas* (*Rv2940c*) genes was carried out by specialized transduction as previously described[29]. H37Rv-B was used to generate H37Rv Δ*tgs1* mutants; H37Rv-SC [a single PDIM(+) clone isolated from H37Rv-B by VAN10-P screening] was used to generate H37Rv Δ*ppsD*; and CDC1551-B to generate CDC1551 Δ*mas* (Supplementary Table 2). Transductants were selected on plates containing hygromycin (75 μg/ml) and the deletion was confirmed by 3-primer PCR and whole genome sequencing (WGS). The Δ*ppsD* strain was complemented using the integrative vector pMV361[57] containing a copy of the *ppsD* gene under control of the HSP60 promoter (pMV361-*ppsD*). The complementation plasmid was constructed by Gibson assembly using the NEBuilder HiFi DNA Assembly Cloning Kit (New England Biolabs). In brief, the plasmid and *ppsD* insert were amplified by PCR and a Gibson assembly reaction was used to transform *Escherichia coli* DH5α. The plasmid was isolated, and the nucleotide sequence of the construct was verified by Sanger sequencing. H37Rv Δ*ppsD* cells were electroporated with ~0.5 μg of the complementation plasmid, recovered overnight in 7H9/OADC/glycerol/tyloxapol at 37 °C with shaking and then selected on plates containing hygromycin (75

μg/ml) and kanamycin (30 μg/ml). The H37Rv Δ*ppsD*::comp strain was validated by PCR to confirm both the complementation and presence of the Δ*ppsD* deletion. Primers used for vector construction and PCR confirmation are listed in Supplementary Table 7.

Thin layer chromatography

Mtb cultures were grown to early log phase and then diluted to OD_{600} 0.3 in 10 ml 7H9/OADC/glycerol/tyloxapol and labelled with propionic acid [1-^{14}C] sodium salt (7 μCi) (American Radiolabeled Chemicals, Inc.). Cultures were incubated with shaking at 37 °C for two days and then spun down. Methanol (2.0 ml), 0.3% sodium chloride aqueous solution (0.2 ml) and petroleum ether (2.0 ml) were added to the cell pellets and the suspensions were vortexed for 30 s followed by centrifugation. The petroleum ether phases were moved to new tubes and the extraction with petroleum ether was repeated twice. The petroleum phases were combined, dried with anhydrous sodium sulfate, filtered and evaporated to dryness under nitrogen. The PDIM extracts were resuspended in dichloromethane (0.2 ml). Counts per minute (cpm) were measured to load approximately 5000 cpm for each sample on a silica gel 60 F254 thin layer chromatography (TLC) plate (Sigma-Aldrich). The TLC plate was eluted three times with petroleum ether/ethyl acetate 98/2. PDIMs were detected by autoradiograph after exposure for 48–72h at -80 °C. PDIM band intensity was quantified using ImageJ (v 1.52a) [58].

MIC assays

Resistance of *Mtb* strains to vancomycin and other inhibitors (Supplementary Table 8) were determined using the microbroth dilution method. Two-fold serial dilutions at 2 × final drug concentration were prepared in standard 7H9/OADC/glycerol/tyloxapol or media supplemented with either 2 × propionate (0.2 or 2.0 mM) or vitamin B_{12} (14.8 μM) at a volume of 100 μl in the inner wells of flat-bottom 96-well plates. The outer wells were aliquoted with 200 μl PBS or media. Strains were precultured in 7H9/OADC/glycerol/tyloxapol to OD_{600} of ~0.8 and then diluted to OD_{600} 0.01 in the same media. 100 μl of the cell dilution was added to plate to give a final OD_{600} of 0.005; 0.1 or 1.0 mM propionate or 7.4 μM vitamin B_{12} for supplemented assays; and 1 × drug concentration. Plates were incubated with gentle shaking and bacterial growth was measured by OD after 10 days unless otherwise specified. For BSL2 strains, OD_{600} was measured on a FLUOstar Omega Microplate Reader (BMG LABTECH). For BSL3 strains, OD_{590} was measured on an Epoch BioTek Microplate Spectrophotometer (BioTek Instruments, Inc.). Data were normalized to drug-free control wells and fit with non-linear regression in Prism (v9.4.1, v10.0.1) (GraphPad Software). MIC_{90} and MIC_{50} values were calculated from the curve fit.

VAN10 assay

VAN10 assays were performed in the inner wells of flat-bottom 96-well plates prepared with standard 7H9/OADC/glycerol/tyloxapol or media supplemented with 2 × propionate (0.2 or 2.0 mM) or vitamin B_{12} (14.8 μM). Triplicate wells were aliquoted with 100 μl drug-free media or media with 20 μg/ml vancomycin. Strains were precultured as for MIC assays and diluted to an OD_{600} of 0.01 in 7H9/OADC/glycerol/tyloxapol. 100 μl of the cell dilution was added to the plate giving a final vancomycin concentration of 10 μg/ml in treated wells (VAN10); OD_{600} of 0.005; and 0.1 or 1.0 mM propionate or 7.4 μM vitamin B_{12} in

supplemented assays. Plates were incubated with gentle shaking and bacterial growth was measured by OD after 10 days unless otherwise specified. Relative growth in VAN10 was calculated compared to drug-free wells (VAN0) (VAN10 OD / VAN0 OD × 100 = VAN10 growth%). The VAN10 assay supplemented with 0.1 mM propionate is referred to as the 'VAN10-P' assay.

For high throughput screening of single colonies and to isolate PDIM(+) clones, single colonies were picked into 7H9/OADC/glycerol/tyloxapol and grown until dense to synchronize. Outgrowth cultures were then subcultured for a single passage and grown to an OD_{600} of ~0.5–1.0. Subcultures were diluted 1:50 in 7H9/OADC/glycerol/tyloxapol and 100 µl of this was used to inoculate VAN10-P assay plates prepared as above. Growth was measured after 14 days to obtain an endpoint measurement. $mc^2$6230 was additionally supplemented with 24 mg/l pantothenate, and 0.1 mM propionate was included in the plates and outgrowth media used to isolate $mc^2$6230 AE1601 (Supplementary Table 1).

Permeability assay

Cell envelope permeability was determined using the Ethidium Bromide (EtBr) uptake assay[16]. Four replicate cultures of *Mtb* $mc^2$7902 and $mc^2$8398 in 10 ml 7H9/OADC/glycerol/ tyloxapol + PALM media were grown to an OD_{600} of 0.6–1.0. Cultures were washed three times with PBS + 0.4% (w/v) glucose and diluted to an OD_{600} of 0.5. Five replicate 180 µl aliquots were transferred to a black, clear-bottom, 96-well plate and 20 µl EtBr (50 µg/ml) was added. The plate was incubated at 37 °C in a FLUOstar Omega Microplate Reader (BMG LABTECH) with 300 rpm double-orbital shaking. Fluorescence was measured at an excitation wavelength of 355 nm and emission wavelength of 590 nm every 15 min for one hour.

Evolution experiments

Triplicate inkwells containing 10 ml standard 7H9/OADC/glycerol/tyloxapol or supplemented media as specified were inoculated with 100 µl of frozen *Mtb* seed stock and incubated for 7–10 days. Cultures were then diluted 1:250 into 10 ml fresh media each week for serial passage. To assess PDIM maintenance over the course of the experiment, at selected passages cultures were input into VAN10-P assays and 1 ml of culture was stocked and stored at -80 °C. VAN10-P assay plates were prepared as above and cultures were diluted 1:100 in 7H9/OADC/glycerol/tyloxapol for input into the assay. Growth was measured after 7 and 14 days of incubation. For TLC lipid analysis of passaged cultures, cultures were first recovered from frozen stocks by growing to an OD_{600} of ~1.0 in standard 7H9/OADC/glycerol/tyloxapol before ^{14}C-labelling and TLC lipid analysis as above.

Metabolomics extractions

Triplicate inkwells containing 7 ml standard 7H9/OADC/glycerol/tyloxapol or supplemented media as specified were inoculated at OD_{600} 0.01 and grown for five days and then harvested. An equivalent of 3 ml culture at an OD_{600} of 1.0 was rapidly filtered on 0.45 µm Durapore PVDF membrane filters (MilliporeSigma) using a vacuum manifold (MilliporeSigma). Cultures were quenched by placing the filter paper in 1 ml of extraction solvent containing 20:40:40 (v/v) water/acetonitrile/methanol with approximately 500 µl

of 0.1 mm zirconia/silica beads (BioSpec) at -20 °C. Samples were homogenized using a Precellys Cryolys Evolution (Bertin Technologies) cooled to 0 °C for three 20 s cycles at 6800 rpm with a 30 s pause between cycles. Samples were centrifuged and the extracts were filtered through a 0.22 μm Nylon Spin-X microcentrifuge filter (Corning) and stored at -80 °C. For analysis, extract samples were concentrated 5-fold by using a SpeedVac® Plus SC110A (Savant Instruments, Inc.) to evaporate the solvent and then redissolved in 1/5th volume of the extraction solvent.

LC-MS metabolomic profiling

Metabolomics analysis was performed using an Agilent 1290 Infinity II liquid chromatography (LC) system coupled with an Agilent 6545 quadrupole time-of-flight (QTOF) mass spectrometer (MS) equipped with a Dual Agilent Jet Stream Electrospray Ionization (Dual AJS ESI) source operated in negative mode. Metabolites were separated on an InfinityLab Poroshell 120 HILIC-Z, 2.1 × 150 mm, 2.7 μm, 100 Å column (Agilent) based on previously described methods[59]. The mobile phase consisted of solvent A: water, and solvent B: 15:85 (v/v) water/acetonitrile, both with 10 mM ammonium acetate and 2.5 μM InfinityLab Deactivator Additive (Agilent), pH 9.0. HPLC grade water (Cen-Med Enterprises) and LC-MS grade solvents (Fisher Chemical) were used for both the LC-MS mobile phase and metabolite extraction. The elution gradient used was as follows: 0–2 min 96% B; 2–5.5 min 96 to 88% B; 5.5–8.5 88% B; 8.5–9 min 88 to 86% B; 9–14 min 86% B; 14–17 min 86 to 82% B; 17–23 min 82 to 65% B; 23–24 min 65% B; 24–24.5 min 64 to 96% B; 24.5–26 min 96% B; followed by a 3 min re-equilibration at 96% B. The flow rate was 0.25 ml/min and column temperature 50 °C. The injection volume was 3 μl and the autosampler was maintained at 4 °C during the run. Mass spectra were recorded in profile mode from m/z 60 to 1200 using an acquisition rate of 1 spectra/s in the 2GHz extended dynamic range mode and 1700 m/z low mass range, using the sensitive slicer mode and fragile ions option. The gas temperature was 225 °C and sheath gas temperature 350 °C. The capillary, nozzle, fragmentor, skimmer, and octopole voltages were 3500, 2000, 125, 45 and 750 V, respectively. Dynamic mass axis calibration was achieved by continuous infusion of a reference mass solution using an isocratic pump with a 100:1 splitter.

Data Analysis was performed using the Agilent MassHunter Qualitative (v10) and Quantitative Analysis Software (v10.1). Metabolite identification was based on mass-retention times determined using chemical standards (Supplementary Fig. 8, Supplementary Table 9) and isotope distribution patterns. Calibration curves of standard compound mixtures in extraction buffer and spiked into a homologous mycobacterial extract were run to determine the linear range. Metabolites were quantified using a mass tolerance of 20 ppm with manual curation of peak areas where necessary and the area under the curve (AUC) was determined. AUC was normalized in Microsoft Excel 365 using the median total AUC for a panel of 50 putative metabolites across different metabolic pathways (Supplementary Table 10) to correct for differences in extraction and concentration efficiency.

Mouse experiments

Mouse experiments were performed in accordance with National Institutes of Health guidelines following the recommendations in the Guide for the Care and Use of Laboratory

Animals[60]. The protocols used in this study were approved by the Institutional Animal Care and Use Committee of Albert Einstein College of Medicine (Protocols #00001445 and #00001332). To generate H37Rv-B, female C57BL/6 mice (Jackson Laboratory) were infected with H37Rv-A via the aerosol route using a 1×10^7 cfu/ml *Mtb* suspension in PBS containing 0.05% tyloxapol and 0.004% antifoam. Mice were sacrificed after 21 days and the lungs homogenized and plated on 7H10/OADC/glycerol plates. All colonies from the lung of a single mouse were harvested and used to inoculate 7H9/OADC/glycerol/tyloxapol in a roller bottle. This was grown to an OD_{600} of 1.8 and then stocked in 1 ml aliquots and stored at -80 °C. To isolate single PDIM(+) clones of Erdman, HN878 and CDC1551, in-house bred $Rag^{-/-}$ mice were infected with 5×10^6 cfu/mouse via the intravenous route. Mice were killed on day 20 post-infection and the lungs homogenized and plated on 7H10/OADC/glycerol plates. Single colonies were picked and outgrown in 7H9/OADC/glycerol/tyloxapol with 0.1 mM propionate for stocking and then subcultured and screened for PDIM using VAN10-P assays as above.

Whole genome sequencing and analysis

Genomic DNA was isolated using a CTAB extraction method as previously described[61] and sequenced in-house on an Illumina MiSeq. Genomic libraries were prepared using the Illumina Nextera XT library preparation kit and sequenced with a 600-cycle v3 reagent kit (2 × 301 bp reads) following the manufacturer's instructions. Genomes with uneven coverage (< 90% of the genome having > 10 × coverage) for which no PDIM SNPs were detected were additionally sequenced with a 150-cycle v3 kit (2 × 76 bp reads) and the data merged for mapping. Additional sequencing by Illumina NextSeq was performed by SeqCenter (Pittsburgh, PA) using the Illumina DNA Prep kit and sequenced on an Illumina NextSeq 2000 (2 × 151 bp reads).

Raw sequence data quality was assessed by FastQC (v0.11.9). Raw reads were trimmed with Trimmomatic (v0.39)[62] using a sliding window quality filter (SLIDINGWINDOW:4:15) and reads less than 25 bp were discarded (MINLEN:25). Trimmed reads were then mapped to the reference genome corresponding to the strain background (H37Rv NC_000962.3, CDC1551 NC_002755.2, Erdman NC_020559.1, HN878 NZ_CM001043.1 and KZN 4207 NC_016768.1) using BWA-MEM (v0.7.17-r1188) (https://github.com/lh3/bwa). Mapping files were sorted and indexed using Samtools (v1.6)[63]. Duplicates were removed using Picard tools (v2.26.10) (http://broadinstitute.github.io/picard) and local realignment was performed using GATK (v.3.8–0)[64]. Mapping quality was assessed using Qualimap (v2.2.1)[65]. Variants were called using Pilon (v1.23)[66] using a minimum depth threshold of 5, base quality threshold of 15 and mapping quality threshold of 40 (--variant --mindepth 5 --minqual 15 --minmq 40). Scripts used for reference-guided assembly and variant calling are available at https://github.com/cvmulholland/MtbShortReadWGS. Variants were annotated using SNPeff (v5.1d)[67]. Geneious Prime® (v2022.2.2) (Biomatters Ltd.) was used to detect low-frequency variants within the PDIM gene region (*tesA–Rv2953*) using the variation/SNP finder feature with a coverage threshold of 10, minimum variant frequency of 10%, and *P* value < 1×10^{-10}. SeqTK (v1.3-r106) (https://github.com/lh3/seqtk) was used to randomly subsample reads for downsampling analyses.

ppsC homopolymeric tract region Sanger sequencing

To identify and confirm mutations in the *ppsC* homopolymeric tract region, a 250 bp fragment encompassing this region was amplified by PCR and then sequenced by Sanger sequencing. PCR was performed in 50 µl reactions containing 2.5 units HOT FIREPol® DNA polymerase (Solis BioDyne), the supplied reaction buffer BD at 1 × concentration, 2.0 mM $MgCl_2$, 250 µM dNTPs, 0.3 µM of each primer, and 2.5% (v/v) DMSO. Primers are listed in Supplementary Table 7. Approximately 25 ng of gDNA was used as the PCR template. Thermal cycling consisted of an initial denaturation and enzyme activation step of 15 min at 95 °C, followed by 35 cycles of 30 s at 95 °C, 45 s at 55 °C, and 30 s at 72 °C. This was followed by a final elongation step of 10 min at 72 °C. PCR products were purified using the Wizard® SV Gel and PCR Clean-Up system (Promega) and then sequenced by Sanger sequencing at GENEWIZ (South Plainfield, NJ) in both the forward and reverse direction using the same primers as for amplification.

Statistical analysis

Statistical analyses were performed using Prism (v9.4.1 and v10.0.) (GraphPad Software). Significant differences were calculated by one- or two-way ANOVA using multiple comparison tests as specified, or the nonparametric Mann-Whitney test for skewed data. Correlations between vancomycin MIC and VAN10 growth% with PDIM were assessed by simple linear regression.

Extended Data

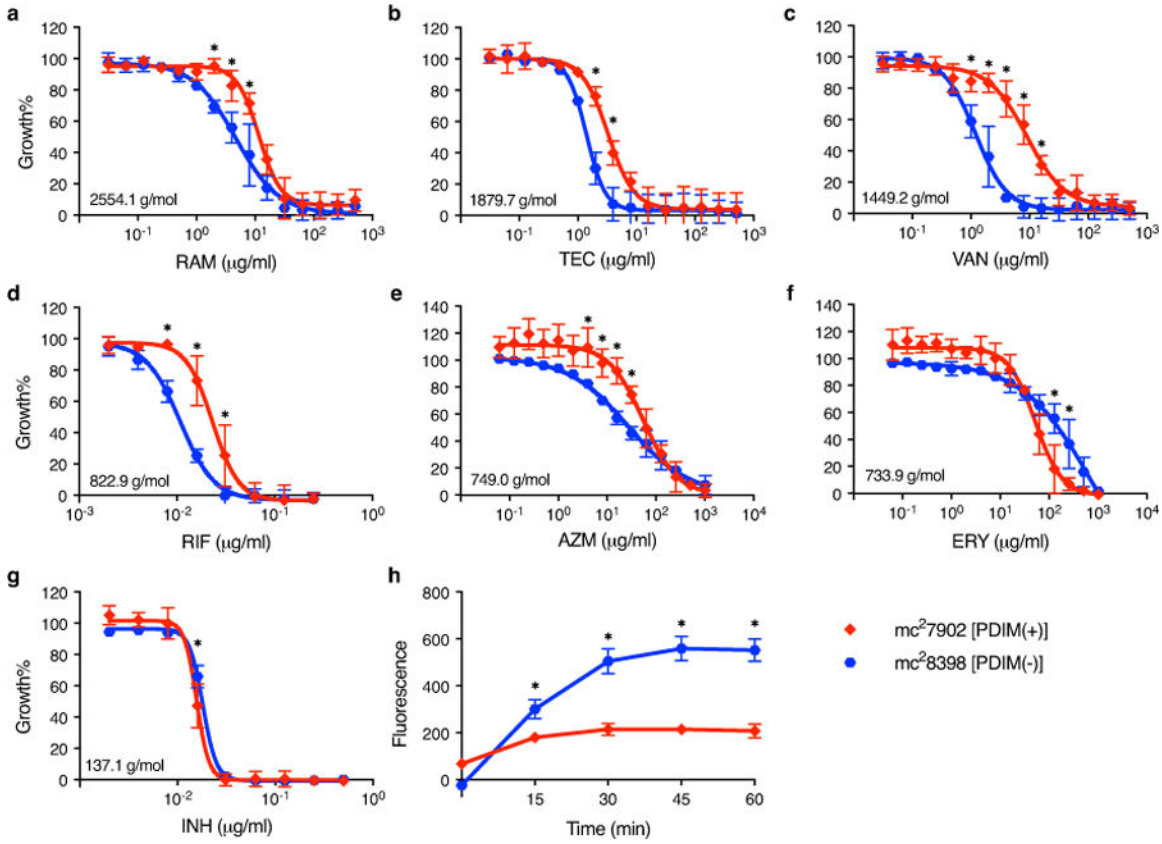

Extended Data Fig. 1. Resistance of PDIM(-) and PDIM(+) *Mtb* to high molecular weight compounds.

a–**g**, MIC assays of *Mtb* mc^{2}7902 [PDIM(+)] and mc^{2}8398 [PDIM(-)] to (**a**) ramoplanin (RAM), (**b**) teicoplanin (TEC), (**c**) vancomycin (VAN), (**d**) rifampicin (RIF), (**e**) azithromycin (AZM), (**f**) erythromycin (ERY), and (**g**) isoniazid (INH). Compounds are arranged by descending molecular weight, which is shown on the MIC plots. MICs were performed in 7H9/OADC/glycerol/tyloxapol + PALM media and bacterial growth was measured after 10 days of incubation and normalized to drug-free controls. Mean ± SD for $n = 4$ biological replicates from two independent experiments. **h**, Ethidium Bromide uptake of mc^{2}7902 and mc^{2}8398. Uptake in whole cell suspensions was monitored by fluorescence (Ex 355 nm/Em 590 nm). Mean ± SD for $n = 4$ biological replicates, each measured in five technical replicates. Uptake data are representative of two independent experiments. $*P < 0.001$; two-way ANOVA with Šidák's multiple comparison test.

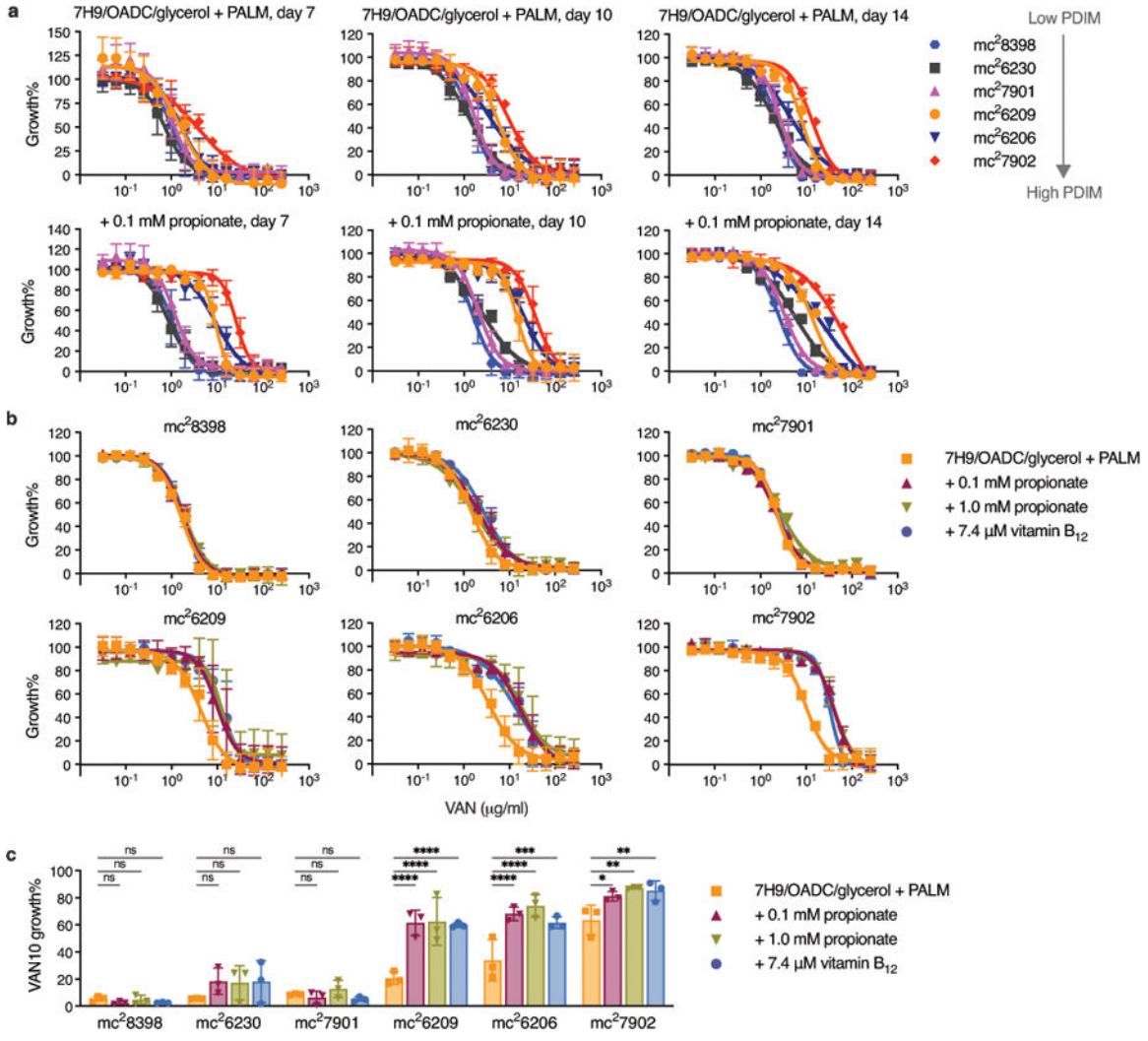

Extended Data Fig. 2. Propionate and vitamin B_{12} supplementation selectively increase vancomycin resistance of PDIM(+) *Mtb* improving assay robustness and reducing time to result.

a, Vancomycin MICs for the PDIM reference strain set in standard 7H9/OADC/glycerol/tyloxapol + PALM media and additionally supplemented with 0.1 mM propionate. Growth was measured after 7, 10, and 14 days as indicated. Mean ± SD for $n = 4$ biological replicates from two independent experiments. **b**, Vancomycin MICs in standard media and additionally supplemented with 0.1 or 1.0 mM propionate or 7.4 µM vitamin B_{12}. Growth was measured after 10 days. Mean ± SD for $n = 4$ biological replicates from two independent experiments. **c**, VAN10 assays in standard and supplemented media. Growth was measured after 10 days. Mean ± SD for $n = 3$ independent experiments, each performed in triplicate. *$P < 0.05$, **$P < 0.01$, ***$P < 0.001$, ****$P < 0.0001$; two-way ANOVA with Šidák's multiple comparison test. The day seven data in (**a**) are also shown in Fig. 1c and are shown here alongside additional time points. The data in (**b**) includes one of the same experiments shown in (**a**), together with data from an independent experiment. The VAN10-P (+ 0.1 mM propionate) data in (**c**) are also shown in Fig. 1e and are shown here alongside additional conditions.

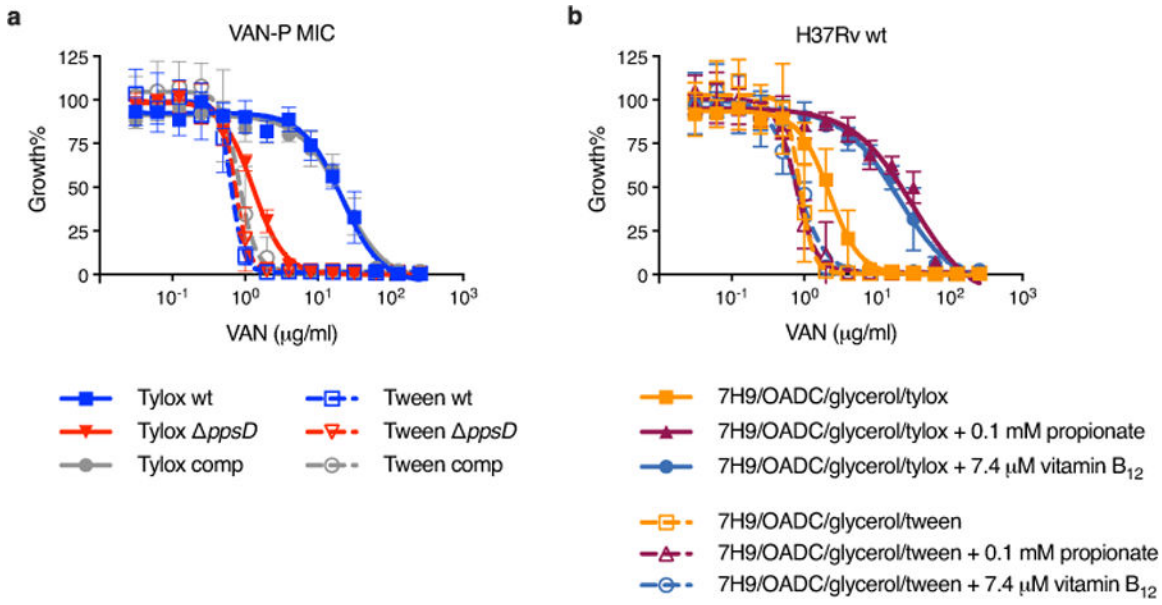

Extended Data Fig. 3. Tween 80 decreases vancomycin resistance and abolishes PDIM-related differences in MIC.

a, VAN-P MICs for PDIM(+) and PDIM(-) *Mtb* H37Rv using either tyloxapol or Tween 80 as the culture detergent. **b**, Vancomycin MICs for PDIM(+) H37Rv wildtype in standard 7H9/OADC/glycerol media and supplemented with propionate or vitamin B_{12} using either tyloxapol or Tween 80 as the detergent. Mean ± SD for $n = 4$ biological replicates from two independent experiments.

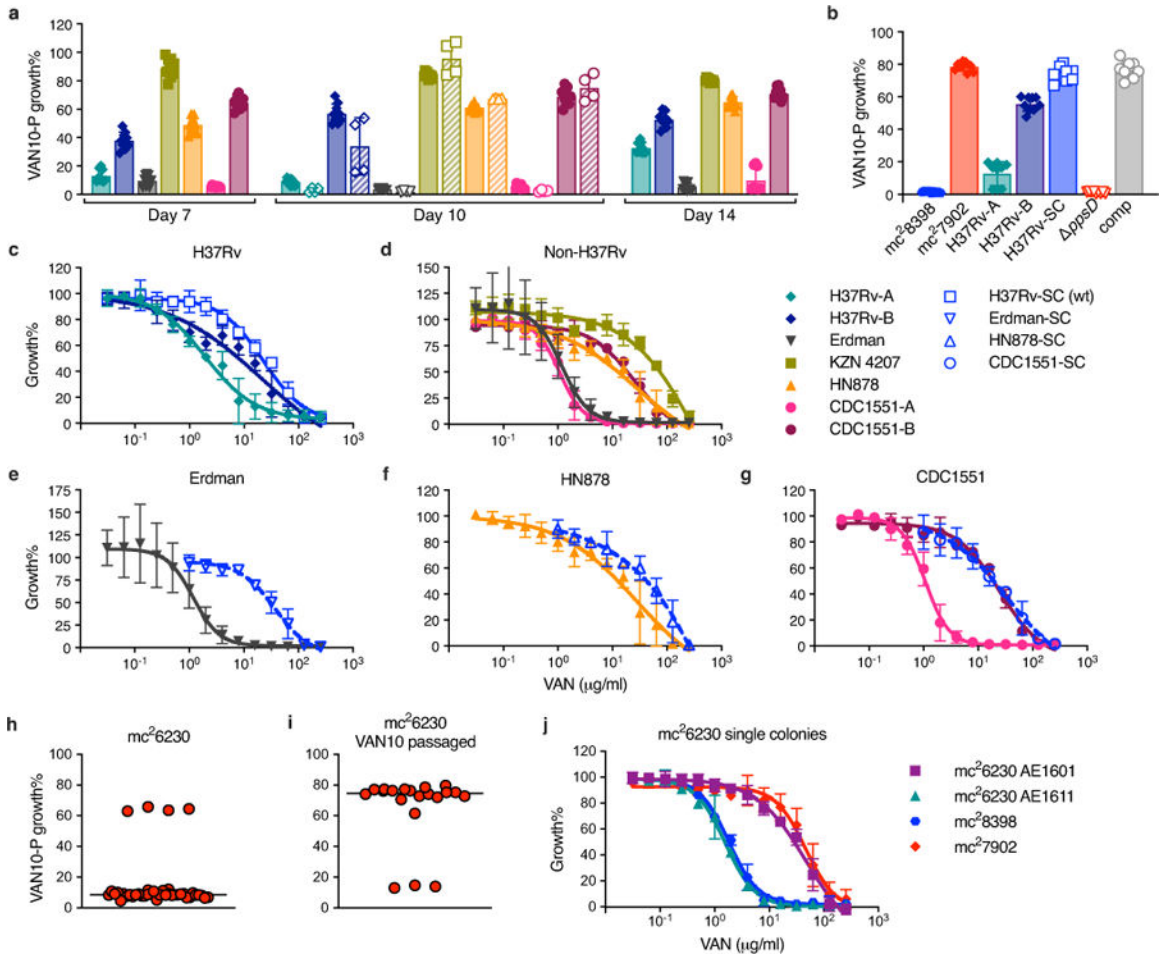

Extended Data Fig. 4. VAN-P assays predict PDIM levels across different *Mtb* strains and lineages and enable re-isolation of single PDIM(+) clones.

a, VAN10-P assays for a range of virulent *Mtb* strains belonging to different lineages. Bacterial growth was measured after 7, 10, and 14 days of incubation as indicated. Data are from the same experiment in Fig. 2a and show additional time points plus an independent experimental repeat measured on day 10 (hatched bars with unfilled symbols). **b**, VAN10-P assays for strains with an H37Rv background including mc^{2}7902 and mc^{2}8398. H37Rv-SC is a single PDIM(+) clone isolated from H37Rv-B by VAN10-P colony screening. This clone was used as our PDIM(+) H37Rv wildtype strain throughout this work and was used to construct H37Rv Δ*ppsD* and Δ*ppsD*::comp mutants (Supplementary Table 2). Data in (**a**,**b**) show mean ± SD for $n = 9$ pairwise comparisons between triplicate wells, except for the day 10 repeat in (**a**) where $n = 4$ pairwise comparisons between duplicate wells. **c**, VAN-P MICs of H37Rv stocks and H37Rv-SC. **d**, VAN-P MICs of non-H37Rv strains from (**a**). **e**–**g**, VAN-P MICs of single PDIM(+) clones isolated from Rag$^{-/-}$ mice using VAN10-P colony screening for (**e**) Erdman, (**f**) HN878, and (**g**) CDC1551 (see also Supplementary Table 3). Data are plotted together with MIC data from (**d**) for comparison. MIC data in (**c**–**g**) show mean ± SD for $n = 4$ biological replicates from two independent experiments. **h**–**j**, Determination that our *Mtb* mc^{2}6230 stock is a mixed population and re-isolation of a single PDIM(+) clone by VAN10-P screening. (**h**) VAN10-P assay of single colonies

isolated from our mc^{2}6230 stock (n = 40) and (**i**) following a single passage in 10 μg/ml vancomycin (n = 20). Vancomycin significantly enriched for PDIM(+) bacilli (P < 0.0001 two-tailed Mann-Whitney test), facilitating re-isolation of low-frequency PDIM(+) clones. Each colony was assayed in triplicate and data points represent mean VAN10-P growth%. Lines indicate the median. **j**, VAN-P MICs of PDIM(+) (AE1601) and PDIM(−) (AE1611) mc^{2}6230 clones identified by VAN10-P colony screening (see also Supplementary Table 3). Mean ± SD for n = 6 biological replicates from two independent experiments.

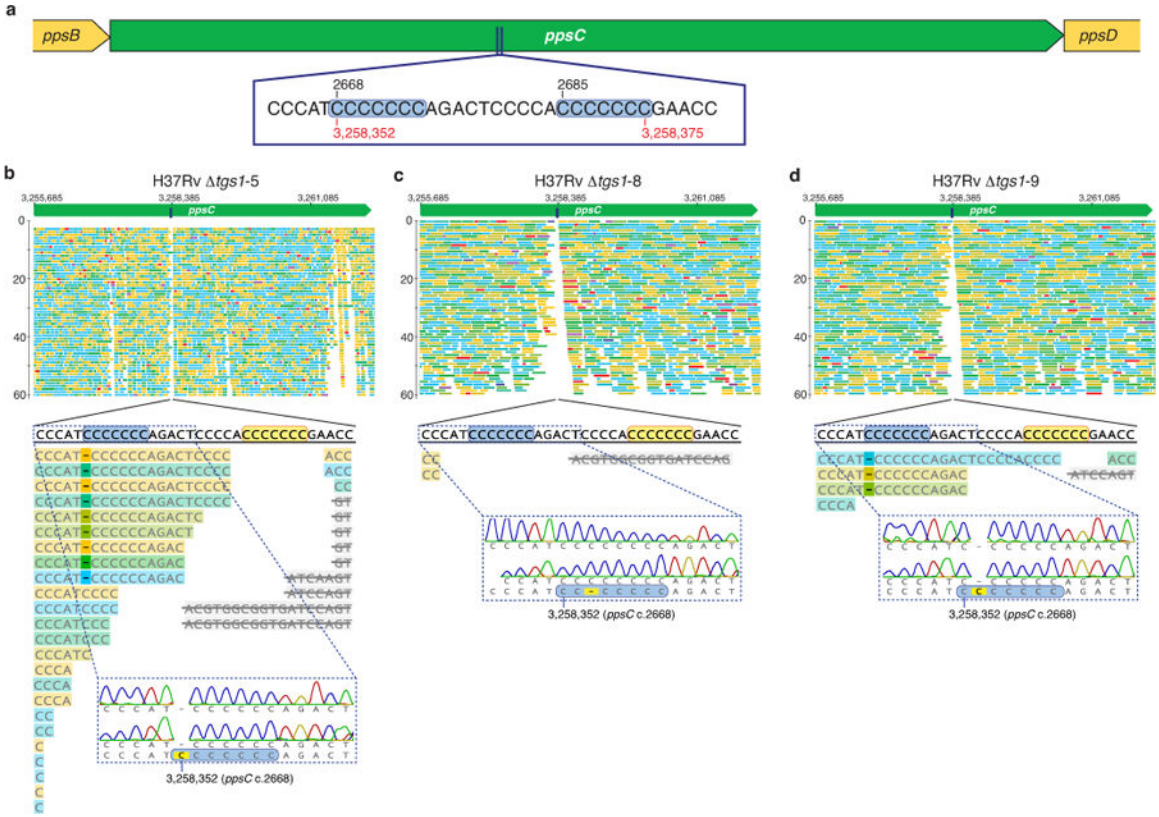

Extended Data Fig. 5. Assessment of *ppsC* homopolymeric tract mutations.

a, Schematic showing the location of a homopolymeric tract region in the *ppsC* gene. Sequence inserts show two adjacent 7-cytosine homopolymeric tracts (c.2668 and c.2685) ± 5 bp on either side. Numbers in black indicate the position in the *ppsC* gene and numbers in red the genomic position in the H37Rv genome. **b**–**d**, Analysis of the *ppsC* homopolymeric tract region in Δ*tgs1* mutants and identification of frameshift mutations. WGS variant calling failed to identify PDIM mutations in Δ*tgs1*-5, Δ*tgs1*-8 and Δ*tgs1*-9 despite a PDIM(-) result in VAN-P MICs (Fig. 2b) and validation of Δ*tgs1*-9 as PDIM(-) by TLC (Fig. 2c). Close manual inspection of WGS reads showed the *ppsC* homopolymeric tract region is poorly covered by Illumina MiSeq and identified potentially missed variant calls. PCR and Sanger sequencing confirmed the presence of a 2668$(C)_{76}$ frameshift mutation in both Δ*tgs1*-5 (**b**) and Δ*tgs1*-9 (**d**) and identified a 2668$(C)_{78}$ mutation in Δ*tgs1*-8 that was not covered at all by WGS (**c**). (**b**–**d**) were created with Geneious Prime® 2022.2.2 and Illustrator 26.4.1. Coverage has been cropped to a read depth of 60 ×. See also Supplementary Table 5.

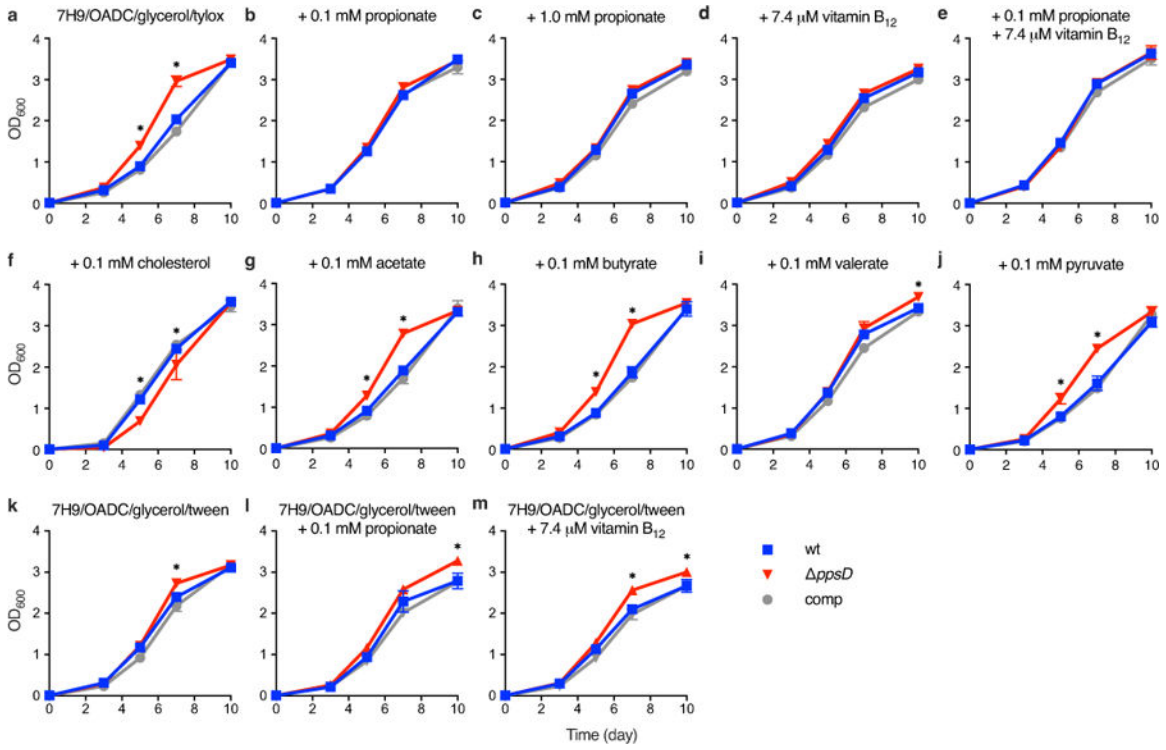

Extended Data Fig. 6. Effect of different media supplements on growth of PDIM(+) and PDIM(−) *Mtb*.

a, Growth of PDIM(+) and PDIM(-) *Mtb* H37Rv in standard 7H9/OADC/glycerol/tyloxapol and **b**–**j**, the same media with additional supplements as indicated. **k**–**m**, Growth using Tween 80 instead of tyloxapol as the culture detergent with additional supplements as indicated. Mean ± SD for $n = 3$ biological replicates. Data are representative of at least two independent experiments. (**a**,**b**,**d**,**f**) show independent experimental repeats for the conditions in Fig. 3. *$P < 0.001$ for both wt and comp versus Δ*ppsD*; two-way ANOVA with Tukey's multiple comparison test. For some data points the SD is smaller than the data symbols.

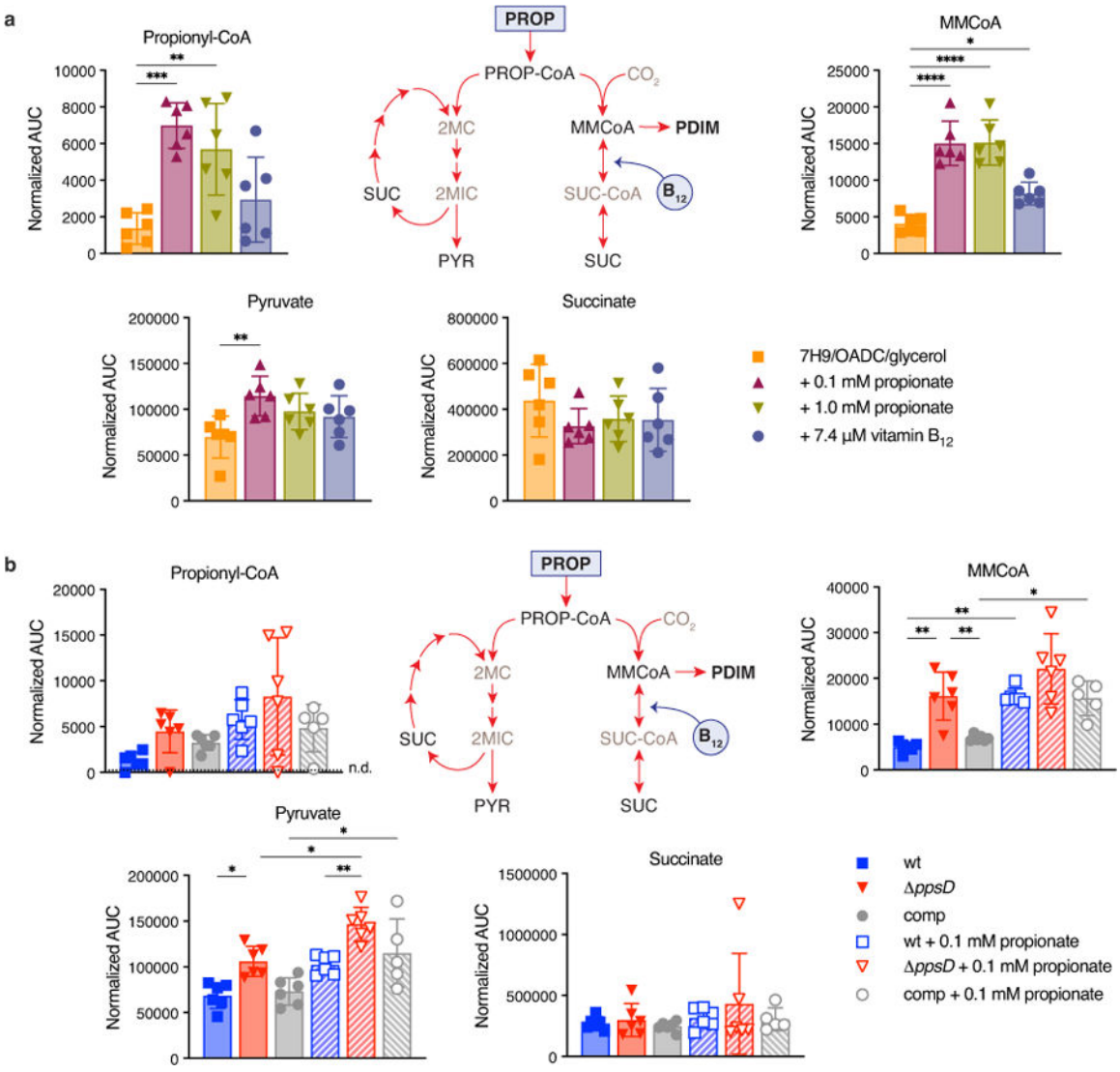

Extended Data Fig. 7. Effects of propionate and vitamin B_{12} supplementation on MMCoA and propionyl-CoA metabolic pathways in *Mtb*.

a, Abundance of metabolites in propionyl-CoA and MMCoA metabolism in PDIM(+) *Mtb* H37Rv wildtype grown in standard 7H9/OADC/glycerol/tyloxapol media and supplemented with propionate or vitamin B_{12}, and **b**, in PDIM(+) and PDIM(-) H37Rv grown in 7H9/OADC/glycerol/tyloxapol ± 0.1 mM propionate. Abundances are shown as normalized area under the curve (AUC) (see Methods). Mean ± SD for $n = 6$ biological replicates from two independent experiments. *$P < 0.05$, **$P < 0.01$, ***$P < 0.001$, ****$P < 0.0001$; one-way ANOVA with Tukey's multiple comparison test. Significant differences compared to unsupplemented media are indicated in (**a**), and between ± propionate for each strain and between strains for each condition in (**b**). PROP, propionate; PROP-CoA, propionyl-CoA; MMCoA, methylmalonyl-CoA; SUC-CoA, succinyl-CoA; SUC, succinate; 2MC/2MIC, 2-methyl(iso)citrate; and PYR, pyruvate. Succinyl-CoA and methyl(iso)citrate were not able to be detected in samples by our method. Propionyl-CoA was close to the detection limit and

was not detected in all samples (n.d. = not detected). The data for MMCoA are also shown in Fig. 3d,e. See also Supplementary Fig. 8.

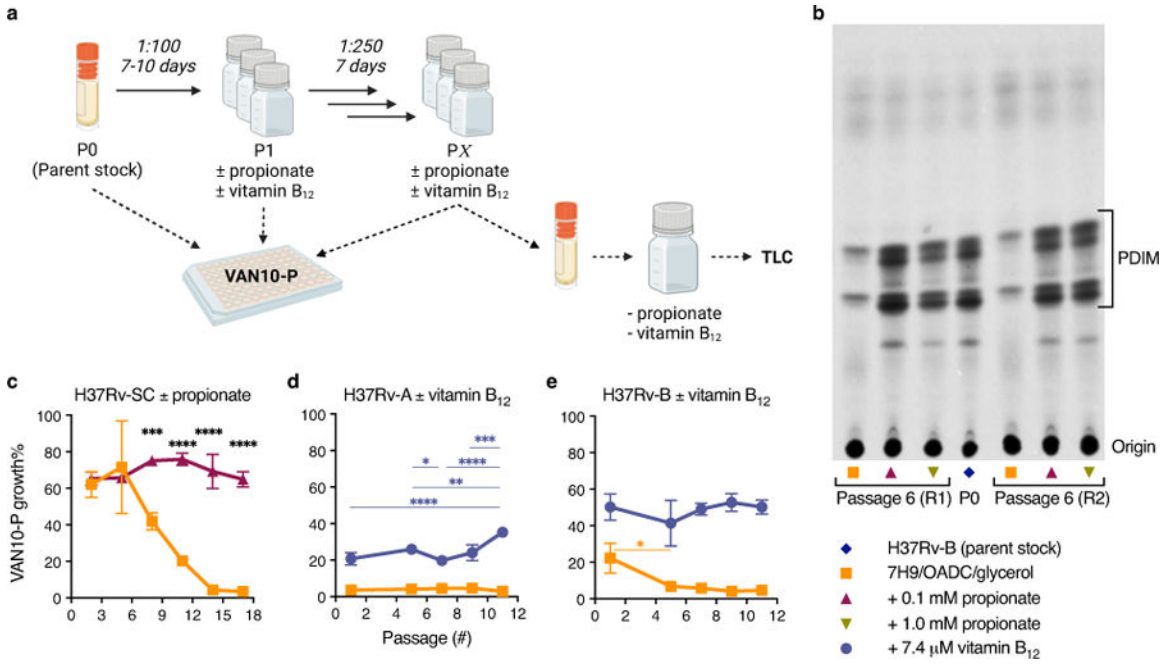

Extended Data Fig. 8. Propionate and vitamin B_{12} supplementation prevent PDIM loss in *Mtb*.
a, Schematic overview of *in vitro* evolution experiments. Triplicate inkwells containing standard 7H9/OADC/glycerol/tyloxapol or media supplemented with propionate or vitamin B_{12} were inoculated with frozen *Mtb* culture stock (P0) and incubated for 7–10 days (P1). Cultures were then diluted into fresh media every 7 days for serial passage (P2 to P*X*). Selected passages were input into VAN10-P assays at the time of passage to assess PDIM production over the course of the experiment. For TLC lipid analysis, frozen stocks were first outgrown in media without propionate or vitamin B_{12} for a single passage to allow the strains to recover before ^{14}C-labelling. Figure created with BioRender.com. **b**, TLC lipid analysis of H37Rv-B before and after six serial passages in ± 0.1 or 1.0 mM propionate. This figure shows the full TLC plate from Fig. 4a with results for both biological replicates analysed by TLC. **c**, VAN10-P assays for H37Rv-SC [PDIM(+) H37Rv wildtype] passaged in ± 0.1 mM propionate. **d**, H37Rv-A and **e**, H37Rv-B passaged in ± 7.4 μM vitamin B_{12}. Mean ± SD for $n = 3$ biological replicates, each assayed in triplicate. *$P < 0.05$, **$P < 0.01$, ***$P < 0.001$, ****$P < 0.0001$; two-way ANOVA with Šidák's (**c**) or Tukey's (**d**,**e**) multiple comparison test. Significant differences between conditions are indicated in (**c**) and between timepoints in (**d**,**e**).

Supplementary Material

Refer to Web version on PubMed Central for supplementary material.

Acknowledgments

We thank Bing Chen, John Kim, and Mei Chen for assistance with animal experiments; Annie Zhi Dai for technical support; Sangeeta Tiwari who constructed the $mc^2$8398 mutant; and the labs of Jeremy Rock, Rockefeller University, NY, and John Chan, Rutgers University, NJ, for their feedback and independent validation of VAN-P PDIM assays. C.V.M., T.J.W., J.C., E.Z.R., and M.B. The authors acknowledge support from the following grants: National Institutes of Health/National Institute of Allergy and Infectious Diseases R01 AI139465 for C.V.M., T.J.W., J.C., E.Z.R., and M.B. , R01 AI175972 for C.V.M., T.J.W., J.C., E.Z.R. and M.B. and AI026170 for C.V., S.R., and W.J.R., the Potts Memorial Foundation for C.V.M., E.Z.R. and M.B., Albert Einstein College of Medicine internal funding for E.Z.R. and M.B., the Institutional AIDS training grant, Training in HIV/AIDS Pathogenesis; Basic and Translational Research (T32 AI007501) for M.W.S., and the Albert Einstein College of Medicine MSTP training grant T32GM149364 for M.W.S..

Data availability statement

Whole genome sequence data have been deposited in the NCBI Sequence Read Archive (SRA) under the BioProject accession number PRJNA923717. A complete list of strains sequenced in this study and SRA accession numbers are given in Supplementary Table 11. Raw metabolomics data are provided as a supplementary data file (Supplementary Data 1). Source data are provided for all Figures and Extended Data Figures.

References

1. Daffe M & Laneelle MA Distribution of phthiocerol diester, phenolic mycosides and related compounds in mycobacteria. J Gen Microbiol 134, 2049–2055 (1988). [PubMed: 3149973]
2. Rens C, Chao JD, Sexton DL, Tocheva EI & Av-Gay Y Roles for phthiocerol dimycocerosate lipids in Mycobacterium tuberculosis pathogenesis. Microbiology (Reading) 167 (2021).
3. Domenech P & Reed MB Rapid and spontaneous loss of phthiocerol dimycocerosate (PDIM) from Mycobacterium tuberculosis grown in vitro: implications for virulence studies. Microbiology (Reading) 155, 3532–3543 (2009). [PubMed: 19661177]
4. Manjunatha UH et al. Identification of a nitroimidazo-oxazine-specific protein involved in PA-824 resistance in Mycobacterium tuberculosis. Proc Natl Acad Sci U S A 103, 431–436 (2006). [PubMed: 16387854]
5. Kirksey MA et al. Spontaneous phthiocerol dimycocerosate-deficient variants of Mycobacterium tuberculosis are susceptible to gamma interferon-mediated immunity. Infect Immun 79, 2829–2838 (2011). [PubMed: 21576344]
6. Cox JS, Chen B, McNeil M & Jacobs WR Jr. Complex lipid determines tissue-specific replication of Mycobacterium tuberculosis in mice. Nature 402, 79–83 (1999). [PubMed: 10573420]
7. Camacho LR, Ensergueix D, Perez E, Gicquel B & Guilhot C Identification of a virulence gene cluster of Mycobacterium tuberculosis by signature-tagged transposon mutagenesis. Mol Microbiol 34, 257–267 (1999). [PubMed: 10564470]
8. Goren MB, Brokl O & Schaefer WB Lipids of putative relevance to virulence in Mycobacterium tuberculosis: phthiocerol dimycocerosate and the attenuation indicator lipid. Infect Immun 9, 150–158 (1974). [PubMed: 4271720]
9. Murry JP, Pandey AK, Sassetti CM & Rubin EJ Phthiocerol dimycocerosate transport is required for resisting interferon-gamma-independent immunity. J Infect Dis 200, 774–782 (2009). [PubMed: 19622047]
10. Day TA et al. Mycobacterium tuberculosis strains lacking surface lipid phthiocerol dimycocerosate are susceptible to killing by an early innate host response. Infect Immun 82, 5214–5222 (2014). [PubMed: 25287926]
11. Rousseau C et al. Production of phthiocerol dimycocerosates protects Mycobacterium tuberculosis from the cidal activity of reactive nitrogen intermediates produced by macrophages and modulates the early immune response to infection. Cell Microbiol 6, 277–287 (2004). [PubMed: 14764111]

12. Wang Q et al. PE/PPE proteins mediate nutrient transport across the outer membrane of Mycobacterium tuberculosis. Science 367, 1147–1151 (2020). [PubMed: 32139546]
13. Camacho LR et al. Analysis of the phthiocerol dimycocerosate locus of Mycobacterium tuberculosis. Evidence that this lipid is involved in the cell wall permeability barrier. J Biol Chem 276, 19845–19854 (2001). [PubMed: 11279114]
14. Tran V, Ahn SK, Ng M, Li M & Liu J Loss of Lipid Virulence Factors Reduces the Efficacy of the BCG Vaccine. Sci Rep 6, 29076 (2016). [PubMed: 27357109]
15. Soetaert K et al. Increased Vancomycin Susceptibility in Mycobacteria: a New Approach To Identify Synergistic Activity against Multidrug-Resistant Mycobacteria. Antimicrob Agents Chemother 59, 5057–5060 (2015). [PubMed: 26033733]
16. Rodrigues L, Viveiros M & Ainsa JA Measuring efflux and permeability in mycobacteria. Methods Mol Biol 1285, 227–239 (2015). [PubMed: 25779319]
17. Jain M et al. Lipidomics reveals control of Mycobacterium tuberculosis virulence lipids via metabolic coupling. Proc Natl Acad Sci U S A 104, 5133–5138 (2007). [PubMed: 17360366]
18. Pandey AK & Sassetti CM Mycobacterial persistence requires the utilization of host cholesterol. Proc Natl Acad Sci U S A 105, 4376–4380 (2008). [PubMed: 18334639]
19. Griffin JE et al. Cholesterol catabolism by Mycobacterium tuberculosis requires transcriptional and metabolic adaptations. Chem Biol 19, 218–227 (2012). [PubMed: 22365605]
20. Gopinath K, Moosa A, Mizrahi V & Warner DF Vitamin B12 metabolism in Mycobacterium tuberculosis. Future Microbiol 8, 1405–1418 (2013). [PubMed: 24199800]
21. Gopinath K et al. A vitamin B12 transporter in Mycobacterium tuberculosis. Open Biol 3, 120175 (2013). [PubMed: 23407640]
22. Savvi S et al. Functional characterization of a vitamin B12-dependent methylmalonyl pathway in Mycobacterium tuberculosis: implications for propionate metabolism during growth on fatty acids. J Bacteriol 190, 3886–3895 (2008). [PubMed: 18375549]
23. Yang X, Nesbitt NM, Dubnau E, Smith I & Sampson NS Cholesterol metabolism increases the metabolic pool of propionate in Mycobacterium tuberculosis. Biochemistry 48, 3819–3821 (2009). [PubMed: 19364125]
24. Koh EI et al. Chemical-genetic interaction mapping links carbon metabolism and cell wall structure to tuberculosis drug efficacy. Proc Natl Acad Sci U S A 119, e2201632119 (2022). [PubMed: 35380903]
25. Quinonez CG et al. The Role of Fatty Acid Metabolism in Drug Tolerance of Mycobacterium tuberculosis. mBio 13, e0355921 (2022). [PubMed: 35012349]
26. Hicks ND et al. Clinically prevalent mutations in Mycobacterium tuberculosis alter propionate metabolism and mediate multidrug tolerance. Nat Microbiol 3, 1032–1042 (2018). [PubMed: 30082724]
27. Wang H et al. An essential bifunctional enzyme in Mycobacterium tuberculosis for itaconate dissimilation and leucine catabolism. Proc Natl Acad Sci U S A 116, 15907–15913 (2019). [PubMed: 31320588]
28. Ortalo-Magne A et al. Identification of the surface-exposed lipids on the cell envelopes of Mycobacterium tuberculosis and other mycobacterial species. J Bacteriol 178, 456–461 (1996). [PubMed: 8550466]
29. Jain P et al. Specialized transduction designed for precise high-throughput unmarked deletions in Mycobacterium tuberculosis. mBio 5, e01245–01214 (2014). [PubMed: 24895308]
30. Dechow SJ, Baker JJ, Murto M & Abramovitch RB ppe51 Variants Enable Growth of Mycobacterium tuberculosis at Acidic pH by Selectively Promoting Glycerol Uptake. J Bacteriol, e0021222 (2022).
31. Gopal P et al. Pyrazinamide Resistance Is Caused by Two Distinct Mechanisms: Prevention of Coenzyme A Depletion and Loss of Virulence Factor Synthesis. ACS Infect Dis 2, 616–626 (2016). [PubMed: 27759369]
32. Orsi RH, Bowen BM & Wiedmann M Homopolymeric tracts represent a general regulatory mechanism in prokaryotes. BMC Genomics 11, 102 (2010). [PubMed: 20144225]
33. Mizrahi V & Andersen SJ DNA repair in Mycobacterium tuberculosis. What have we learnt from the genome sequence? Mol Microbiol 29, 1331–1339 (1998). [PubMed: 9781872]

34. Dolan SK et al. Loving the poison: the methylcitrate cycle and bacterial pathogenesis. Microbiology (Reading) 164, 251–259 (2018). [PubMed: 29458664]
35. Munoz-Elias EJ, Upton AM, Cherian J & McKinney JD Role of the methylcitrate cycle in Mycobacterium tuberculosis metabolism, intracellular growth, and virulence. Mol Microbiol 60, 1109–1122 (2006). [PubMed: 16689789]
36. Lee W, VanderVen BC, Fahey RJ & Russell DG Intracellular Mycobacterium tuberculosis exploits host-derived fatty acids to limit metabolic stress. J Biol Chem 288, 6788–6800 (2013). [PubMed: 23306194]
37. Singh A et al. Mycobacterium tuberculosis WhiB3 maintains redox homeostasis by regulating virulence lipid anabolism to modulate macrophage response. PLoS Pathog 5, e1000545 (2009). [PubMed: 19680450]
38. Lu R et al. Catabolism of the Cholesterol Side Chain in Mycobacterium tuberculosis Is Controlled by a Redox-Sensitive Thiol Switch. ACS Infect Dis 3, 666–675 (2017). [PubMed: 28786661]
39. Eoh H & Rhee KY Methylcitrate cycle defines the bactericidal essentiality of isocitrate lyase for survival of Mycobacterium tuberculosis on fatty acids. Proc Natl Acad Sci U S A 111, 4976–4981 (2014). [PubMed: 24639517]
40. Dulberger CL, Rubin EJ & Boutte CC The mycobacterial cell envelope - a moving target. Nat Rev Microbiol 18, 47–59 (2020). [PubMed: 31728063]
41. Marrero J, Rhee KY, Schnappinger D, Pethe K & Ehrt S Gluconeogenic carbon flow of tricarboxylic acid cycle intermediates is critical for Mycobacterium tuberculosis to establish and maintain infection. Proc Natl Acad Sci U S A 107, 9819–9824 (2010). [PubMed: 20439709]
42. Block AM et al. Mycobacterium tuberculosis Requires the Outer Membrane Lipid Phthiocerol Dimycocerosate for Starvation-Induced Antibiotic Tolerance. mSystems 8, e0069922 (2023). [PubMed: 36598240]
43. Maksymiuk C et al. Comparison of transposon and deletion mutants in Mycobacterium tuberculosis: The case of rv1248c, encoding 2-hydroxy-3-oxoadipate synthase. Tuberculosis (Edinb) 95, 689–694 (2015). [PubMed: 26547230]
44. Chen JM, Islam ST, Ren H & Liu J Differential productions of lipid virulence factors among BCG vaccine strains and implications on BCG safety. Vaccine 25, 8114–8122 (2007). [PubMed: 17954004]
45. Bloch H & Segal W Biochemical differentiation of Mycobacterium tuberculosis grown in vivo and in vitro. J Bacteriol 72, 132–141 (1956). [PubMed: 13366889]
46. Babunovic GH et al. CRISPR Interference Reveals That All-Trans-Retinoic Acid Promotes Macrophage Control of Mycobacterium tuberculosis by Limiting Bacterial Access to Cholesterol and Propionyl Coenzyme A. mBio 13, e0368321 (2022). [PubMed: 35038923]
47. Dubos RJ & Middlebrook G Media for tubercle bacilli. Am Rev Tuberc 56, 334–345 (1947). [PubMed: 20270481]
48. Dubos RJ Rapid and submerged growth of mycobacteria in liquid media. Proc Soc Exp Biol Med 58, 361–362 (1945).
49. Li S et al. CRISPRi chemical genetics and comparative genomics identify genes mediating drug potency in Mycobacterium tuberculosis. Nat Microbiol 7, 766–779 (2022). [PubMed: 35637331]
50. Xu W et al. Chemical Genetic Interaction Profiling Reveals Determinants of Intrinsic Antibiotic Resistance in Mycobacterium tuberculosis. Antimicrob Agents Chemother 61 (2017).
51. Chengalroyen MD et al. DNA-Dependent Binding of Nargenicin to DnaE1 Inhibits Replication in Mycobacterium tuberculosis. ACS Infect Dis 8, 612–625 (2022). [PubMed: 35143160]
52. Wang Q & Boshoff HI M. Determining Minimum Inhibitory Concentrations in Liquid Cultures or on Solid Medium. Methods Mol Biol 2314, 595–609 (2021). [PubMed: 34235672]
53. Chandra P, Grigsby SJ & Philips JA Immune evasion and provocation by Mycobacterium tuberculosis. Nat Rev Microbiol 20, 750–766 (2022). [PubMed: 35879556]
54. DeJesus MA et al. Comprehensive Essentiality Analysis of the Mycobacterium tuberculosis Genome via Saturating Transposon Mutagenesis. mBio 8 (2017).
55. Bosch B et al. Genome-wide gene expression tuning reveals diverse vulnerabilities of M. tuberculosis. Cell 184, 4579–4592 e4524 (2021). [PubMed: 34297925]

56. Zhang YJ et al. Tryptophan biosynthesis protects mycobacteria from CD4 T-cell-mediated killing. Cell 155, 1296–1308 (2013). [PubMed: 24315099]
57. Stover CK et al. New use of BCG for recombinant vaccines. Nature 351, 456–460 (1991). [PubMed: 1904554]
58. Schneider CA, Rasband WS & Eliceiri KW NIH Image to ImageJ: 25 years of image analysis. Nat Methods 9, 671–675 (2012). [PubMed: 22930834]
59. Dai Y & Hsiao JJ Discovery Metabolomics LC/MS Methods Optimized for Polar Metabolites. Application note, Agilent Technologies, Inc (2019).
60. National Research Council of the National Academies. Guide for the Care and Use of Laboratory Animals: Eighth Edition. (National Academies Press, 2011).
61. Wilson K Preparation of genomic DNA from bacteria. Curr Protoc Mol Biol 56, 2.4.1–2.4.5 (2001).
62. Bolger AM, Lohse M & Usadel B Trimmomatic: a flexible trimmer for Illumina sequence data. Bioinformatics 30, 2114–2120 (2014). [PubMed: 24695404]
63. Danecek P et al. Twelve years of SAMtools and BCFtools. Gigascience 10 (2021).
64. DePristo MA et al. A framework for variation discovery and genotyping using next-generation DNA sequencing data. Nat Genet 43, 491–498 (2011). [PubMed: 21478889]
65. Okonechnikov K, Conesa A & Garcia-Alcalde F Qualimap 2: advanced multi-sample quality control for high-throughput sequencing data. Bioinformatics 32, 292–294 (2016). [PubMed: 26428292]
66. Walker BJ et al. Pilon: an integrated tool for comprehensive microbial variant detection and genome assembly improvement. PLoS One 9, e112963 (2014). [PubMed: 25409509]
67. Cingolani P et al. A program for annotating and predicting the effects of single nucleotide polymorphisms, SnpEff: SNPs in the genome of Drosophila melanogaster strain w1118; iso-2; iso-3. Fly (Austin) 6, 80–92 (2012). [PubMed: 22728672]
68. Sambandamurthy VK et al. Mycobacterium tuberculosis DeltaRD1 DeltapanCD: a safe and limited replicating mutant strain that protects immunocompetent and immunocompromised mice against experimental tuberculosis. Vaccine 24, 6309–6320 (2006). [PubMed: 16860907]
69. Jain P et al. phi(2)GFP10, a high-intensity fluorophage, enables detection and rapid drug susceptibility testing of Mycobacterium tuberculosis directly from sputum samples. J Clin Microbiol 50, 1362–1369 (2012). [PubMed: 22278833]
70. Vilcheze C et al. Rational Design of Biosafety Level 2-Approved, Multidrug-Resistant Strains of Mycobacterium tuberculosis through Nutrient Auxotrophy. mBio 9 (2018).
71. Jacobs WR Jr. & Tiwari S Double auxotrophic and uses thereof. U.S. patent 11666648 (2023).

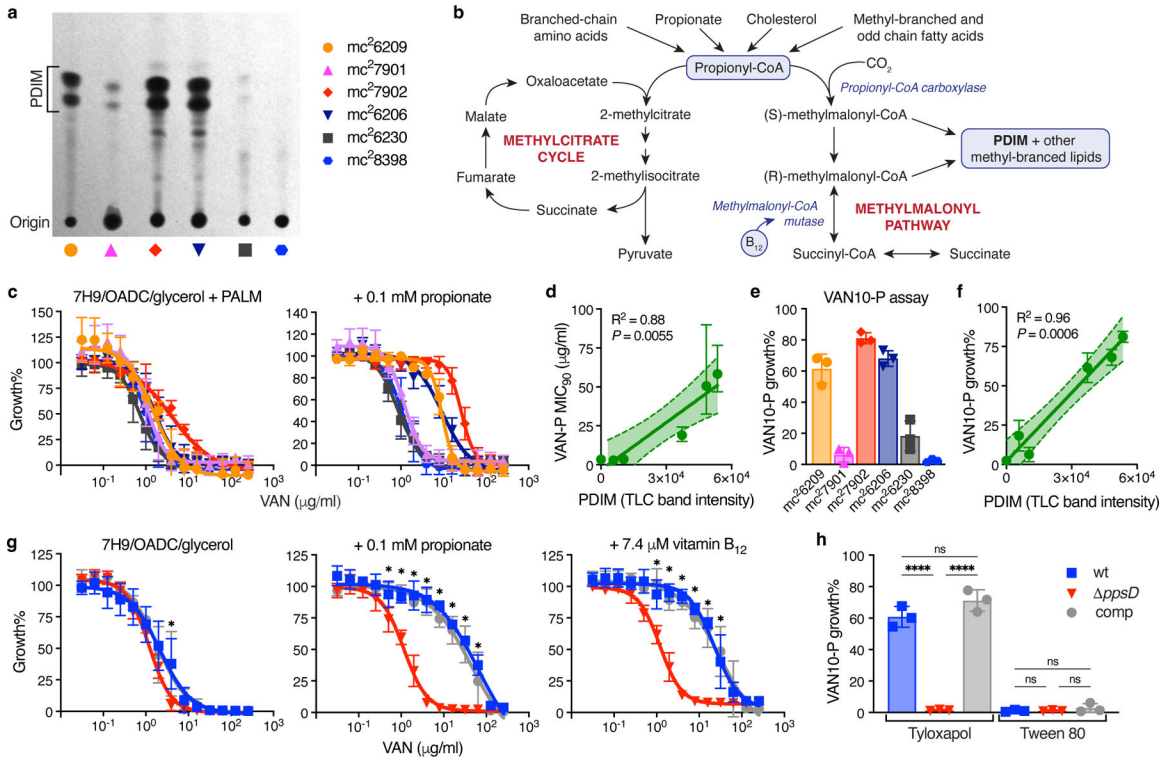

Fig. 1 |. Vancomycin resistance is enhanced by propionate or vitamin B_{12} supplementation and is predictive of PDIM production in *Mtb*.

a, TLC lipid analysis of the PDIM reference strain set (see Supplementary Table 1). **b**, Metabolic pathways of methylmalonyl-CoA production and propionyl-CoA catabolism. **c**, Vancomycin resistance of the *Mtb* PDIM reference strain set in 7H9/OADC/glycerol/tyloxapol + PALM (pantothenate, arginine, leucine, and methionine) media, and additionally supplemented with 0.1 mM propionate ('VAN-P' MIC), measured after 7 days incubation. **d**, Correlation between VAN-P MIC_{90} from the curve fit in (**c**) (+ 0.1 mM propionate) and PDIM band intensity from (**a**). The solid line indicates the linear regression best-fit, and the error bands the 95% CI. **e**, 'VAN10-P' assay comparing growth in 10 μg/ml vancomycin with 0.1 mM propionate to drug-free controls (VAN10 OD / VAN0 OD × 100 = VAN10-P growth%). **f**, Correlation between VAN10-P growth% from (**e**) and PDIM from (**a**). The solid line indicates the linear regression best-fit, and the error bands the 95% CI. **g**, Vancomycin resistance of PDIM(+) and PDIM(-) *Mtb* H37Rv strains in standard 7H9/OADC/glycerol/tyloxapol media and supplemented with 0.1 mM propionate or 7.4 μM vitamin B_{12} (10 μg/ml). *$P < 0.001$ for both wt and comp versus Δ*ppsD*; two-way ANOVA with Tukey's multiple comparison test. **h**, VAN10-P assay of H37Rv strains with tyloxapol or Tween 80. ****$P < 0.0001$; one-way ANOVA with Tukey's multiple comparison test. MIC data show mean ± SD for $n = 4$ biological replicates from two independent experiments. VAN10-P data show mean ± SD for $n = 3$ three independent experiments, each performed in triplicate.

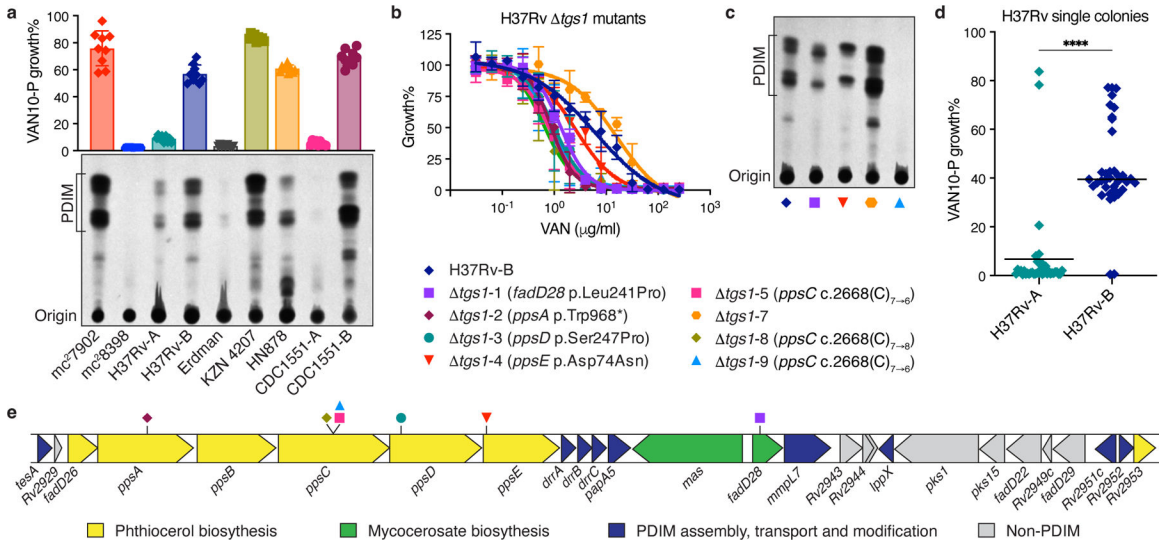

Fig. 2 |. VAN-P assays accurately predict PDIM status during genetic manipulations and across different *Mtb* strains and lineages.

a, TLC lipid analysis and VAN10-P assays of different laboratory stocks of virulent *Mtb* strains alongside *Mtb* mc^{2}7902 and mc^{2}8398. Mean ± SD for $n = 9$ pairwise comparisons between triplicate wells. **b**, VAN-P MIC assays of eight Δ*tgs1* mutants and the parent H37Rv-B. Mean ± SD for $n = 3$ (Δ*tgs1*-3, -5, -7 and -9) or $n = 4$ (H37Rv-B, Δ*tgs1*-1, -2, -4, -8) biological replicates from two independent experiments. Mutations in PDIM biosynthetic genes are indicated in brackets in the legend. No mutations were detected in H37Rv-B or Δ*tgs1*-7. **c**, TLC lipid analysis of four Δ*tgs1* mutants and H37Rv-B. Lipid extracts in (**a**) and (**c**) were run on the same TLC plate. **d**, VAN10-P screening of single colonies isolated from H37Rv-A ($n = 38$) and H37Rv-B ($n = 37$). Each colony was assayed in triplicate and data points represent mean VAN10-P growth%. Lines indicate the median. $P < 0.0001$; unpaired two-tailed Mann-Whitney test. **e.** Schematic showing the PDIM gene cluster and location of secondary PDIM mutations in Δ*tgs1* mutants.

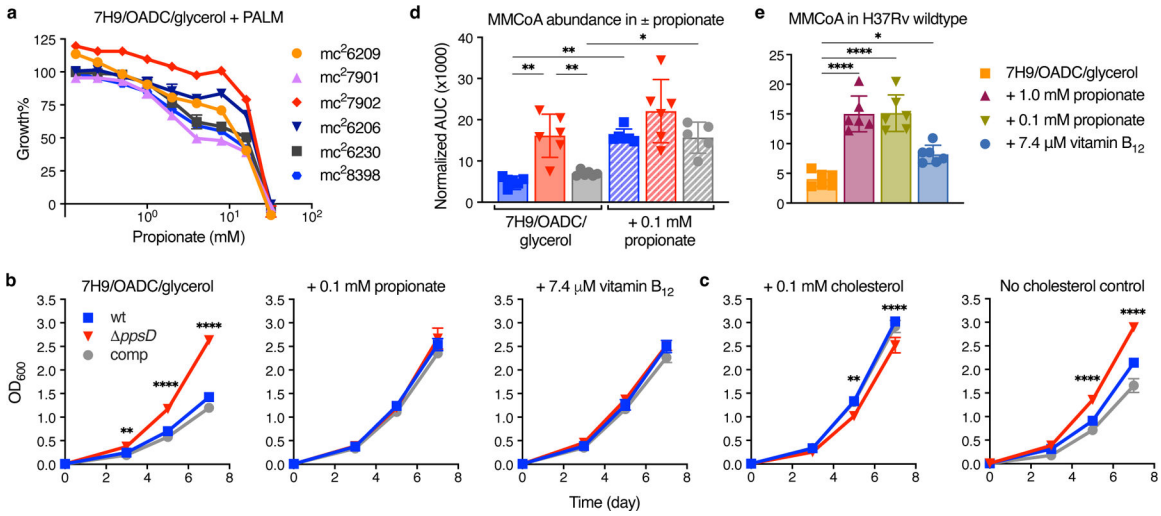

Fig. 3 |. Propionate and vitamin B_{12} supplementation restore the growth of PDIM(+) *Mtb*.

a, Relative growth of the PDIM reference strain set in 7H9/OADC/glycerol/tyloxapol + PALM media with increasing concentrations of propionate compared to no propionate controls. Mean ± SD for $n = 3$ biological replicates. **b**, Growth curves of PDIM(+) and PDIM(−) *Mtb* H37Rv in standard 7H9/OADC/glycerol/tyloxapol media and supplemented with 0.1 mM propionate or 7.4 µM vitamin B_{12} (10 µg/ml). **c**, Growth in 7H9/OADC/glycerol/tyloxapol media + 0.1 mM cholesterol and no cholesterol controls (see Methods). The growth of Δ*ppsD* was significantly lower in cholesterol compared to the no cholesterol control ($P < 0.0001$; days 7 and 10). Mean ± SD for $n = 3$ biological replicates. $^{**}P < 0.01$, $^{****}P < 0.0001$ for both wt and comp versus Δ*ppsD*; two-way ANOVA with Šidák's multiple comparison test. Data in (**a**–**c**) are representative of at least two independent experiments. For some data points the SD is smaller than the data symbols. **d**, Abundance of methylmalonyl-CoA (MMCoA) in PDIM(+) and PDIM(-) H37Rv grown in standard 7H9/OADC/glycerol/tyloxapol media ± 0.1 mM propionate, and **e**, PDIM(+) H37Rv wildtype in standard media and supplemented with either propionate or vitamin B_{12}. The legend for (**d**) is the same as that for (**b**–**c**). Abundances are shown as normalized area under the curve (AUC) (see Methods). Mean ± SD for $n = 6$ biological replicates from two independent experiments. $^{*}P < 0.05$, $^{**}P < 0.01$, $^{****}P < 0.0001$; one-way ANOVA with Tukey's multiple comparison test. Significant differences between ± propionate for each strain and between strains for each condition are indicated in (**d**), and compared to unsupplemented media in (**e**).

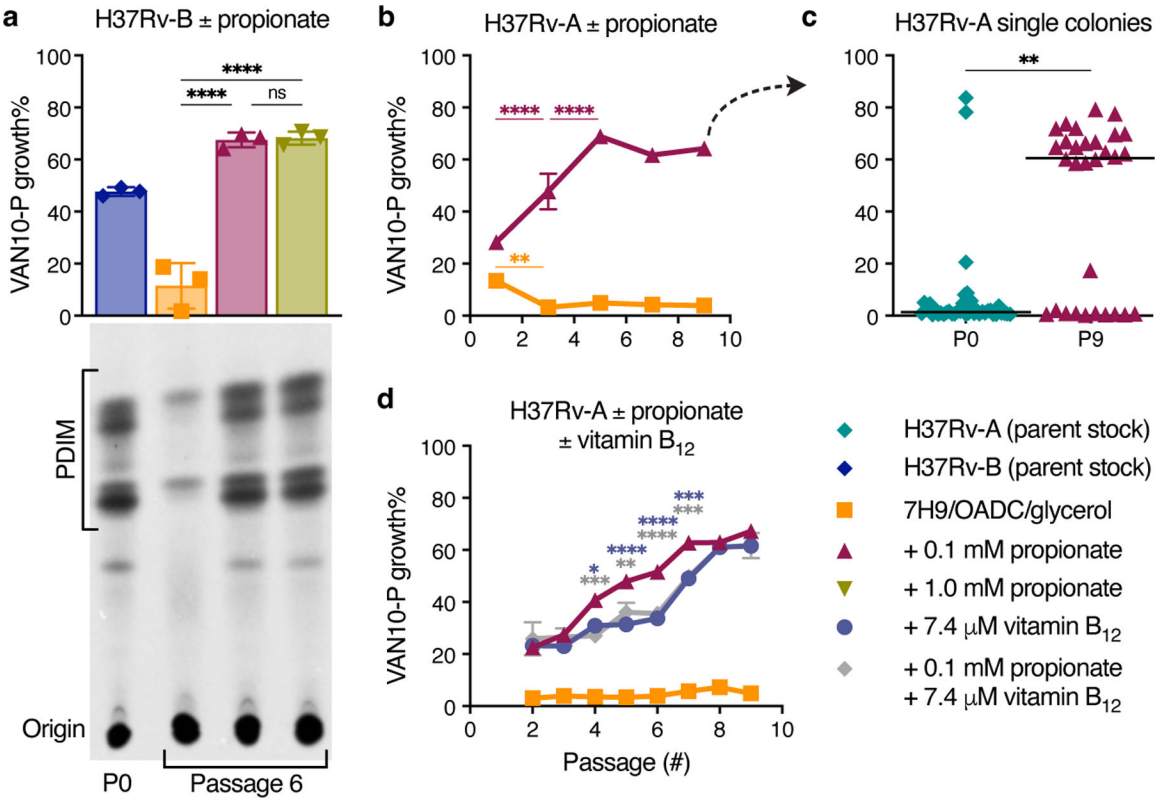

Fig. 4 |. Propionate and vitamin B_{12} supplementation prevent PDIM loss in *Mtb*.

a, VAN10-P and TLC lipid analysis of PDIM levels in *Mtb* H37Rv-B following serial passage in 7H9/OADC/glycerol/tyloxapol media ± 0.1 or 1.0 mM propionate. ****$P <$ 0.0001; one-way ANOVA with Tukey's multiple comparison test. A representative result is shown for one of two biological replicates analysed by TLC (see also Extended Data Fig. 8b). **b**, VAN10-P assays of H37Rv-A passaged in ± 0.1 mM propionate. Significant differences between successive timepoints for each condition are indicated (**$P < 0.01$, ****$P < 0.0001$); two-way ANOVA with Tukey's multiple comparison test. **c**, VAN10-P screening of single colonies of H37Rv-A before ($n = 38$; same data as Fig. 2d) and after propionate passage in (**b**) ($n = 30$). Each colony was assayed in triplicate and data points represent mean VAN10-P growth%. Lines indicate the median. $P = 0.0047$; unpaired two-tailed Mann-Whitney test. **d**, VAN10-P assays of H37Rv-A passaged in media supplemented with ± 0.1 mM propionate and 7.4 μM vitamin B_{12} (10 μg/ml) alone and in combination. Significant differences compared to + 0.1 mM propionate are indicated (*$P < 0.05$, **$P <$ 0.01, ***$P < 0.001$, ****$P < 0.0001$); two-way ANOVA with Tukey's multiple comparison test. $P > 0.05$ for vitamin B_{12} versus vitamin B_{12} + propionate and $P < 0.0001$ for standard media versus each supplemented condition at all timepoints. VAN10-P data in (**a**,**b**,**d**) show mean ± SD for $n = 3$ biological replicates, each assayed in triplicate. For some data points the SD is smaller than the data symbols.

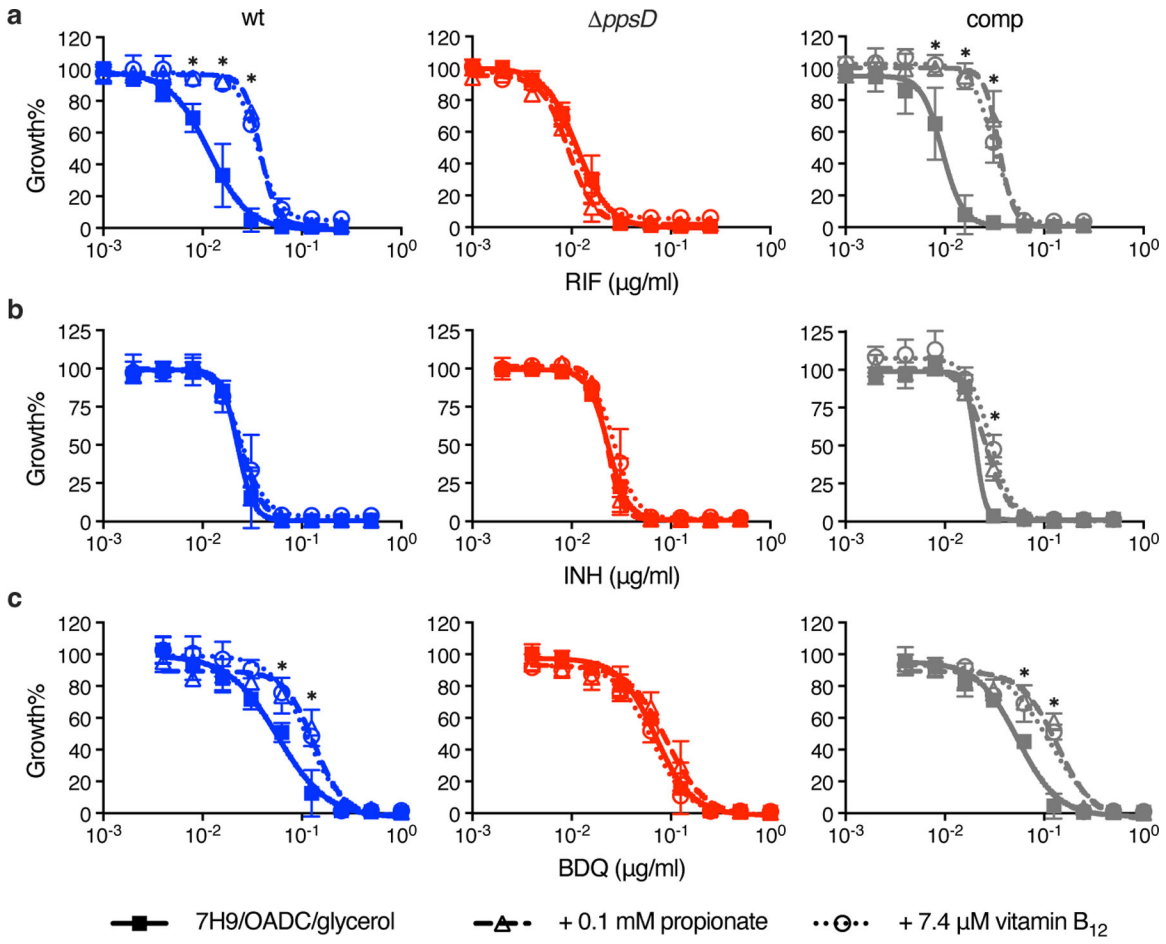

Fig. 5 |. Propionate and vitamin B_{12} supplementation increase rifampicin and bedaquiline resistance of *Mtb* in a PDIM-dependent manner.

Sensitivity of PDIM(+) and PDIM(-) *Mtb* H37Rv to **a**, rifampicin (RIF), **b**, isoniazid (INH), and **c**, bedaquiline (BDQ), in standard 7H9/OADC/glycerol/tyloxapol media and supplemented with either 0.1 mM propionate or 7.4 μM vitamin B_{12} (10 μg/ml). $*P < 0.001$ for both propionate and vitamin B_{12} versus unsupplemented; two-way ANOVA with Tukey's multiple comparison test. Mean ± SD for $n = 4$ biological replicates from two independent experiments.

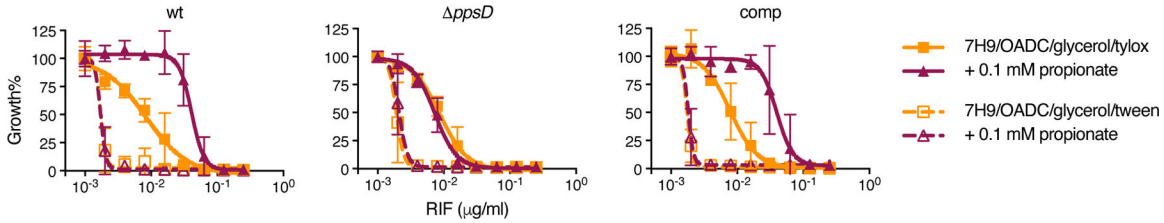

Fig. 6 |. Tween 80 increases the sensitivity of *Mtb* to rifampicin and abolishes PDIM-dependent differences in MIC.

Sensitivity of PDIM(+) and PDIM(-) *Mtb* H37Rv to rifampicin (RIF) in 7H9/OADC/glycerol media ± 0.1 mM propionate using either tyloxapol or Tween 80 as the culture detergent. Mean ± SD for $n = 4$ biological replicates from two independent experiments.